DURABILITY AND DEGRADATION OF HT9 BASED ALLOY WASTE FORMS WITH VARIABLE NI AND CR CONTENT

Fuel Cycle Research & Development

SUMMARY

Short-term electrochemical and long-term hybrid electrochemical corrosion tests were performed on alloy waste forms in reference aqueous solutions that bound postulated repository conditions. The alloy waste forms investigated represent candidate formulations that can be produced with advanced electrochemical treatment of used nuclear fuel. The studies helped to better understand the alloy waste form durability with differing concentrations of nickel and chromium, species that can be added to alloy waste forms to potentially increase their durability and decrease radionuclide release into the environment.

Surrogate alloy waste forms were made into electrodes and electrochemically tested in reference alkaline and acidic brines. A corrosion test protocol was developed in collaboration with Argonne National Laboratory, and consisted of 4 main steps, 1) measure the bare surface corrosion behavior in reference solutions centered at the open circuit potential over a wide imposed potential range, 2) perform several differing potentiostatic holds to measure the time-evolution of anodic current, evolution of surface properties, and radionuclide concentrations in solution, 3) relate steady-state current to radionuclide (or surrogate) specie release rates through periodic sampling of test electrolyte, and 4) identify the corroding phase/phases using SEM/EDS. This combined electrochemical with extended immersion testing is referred to as hybrid electrochemical corrosion testing.

The waste forms were based on the RAW-6 composition, consisting primarily of HT9 steel and other elemental additions to simulate nuclear fuel reprocessing waste. Previous work had shown RAW made with 316 SS to be very corrosion resistant, and the RAW-6 compositions were intended to investigate whether adding Ni and Cr to an alloy made with HT9 could reproduce this level of corrosion resistance. The added Ni will report to a Zr-Fe phase in the alloy forms that hosts the actinides (e.g. U), whereas the Cr will generally report to an Fe-rich(Fe-Cr) phase that in previous studies was found to host the Re (or Tc surrogate). SRNL examined 3 modifications of the RAW-6 formulation, with each variation having a different Cr and Ni content. The solution conditions were at a nominal pH from pH 3 to pH 10. The alloy electrode surface conditions evolved from an initial fresh polish to an oxide during the testing. The corrosion behavior of alloy RAW-6(Ni3) was examined in depth at pH 3 using hybrid electrochemical testing, in which the electrochemical potential was held at a specific oxidative or reducing value while monitoring the current, for periods up to a week. Electrochemical impedance measurements were periodically taken during the hybrid testing to characterize the formation of a passivation layer.

The corrosion results and corrosion parameters derived therefrom will be integrated into an analytical oxidative-dissolution model, in development at Argonne National Laboratory, to calculate radionuclide release rates from the waste form under its evolution in surface condition with aqueous exposure.

The short term fresh surface electrochemical testing and microstructural characterization using SEM/EDS indicated that the RAW-6(Ni3) alloy had the largest passive region in the test solutions. This alloy was examined in depth with hybrid testing and solution sampling. The evolution of the open circuit corrosion potential was also investigated for RAW-6(Ni3), and it

was found that a value of -450 mV vs SCE would result in a transition from oxidative to reducing conditions within less than an hour, but not at more oxidative potentials.

The hybrid testing imposed potentials placed the alloy in one of three separation corrosion conditions: reducing conditions; active-passive conditions; and in the transpassive region. Changes in solution chemistry during the hybrid tests at the different imposed potentials were minimal, with an exception being the hold potential in the transpassive region, which experienced significant release of the majority of the alloying elements monitored for, such as Mo and Re (surrogates for Tc).

SEM/EDS provided evidence of localized corrosion of the high-Zr phases that are the predominant phases containing the U. No evidence of high localized corrosion of the steel phases was observed. This indicates general uniform corrosion was likely occurring on the steel phases if corrosion was occurring, or that the oxide passivation layer was protective of the mostly Fe-Cr phase. The alloy held at transpassive potentials experienced localized corrosion in the Zr-Fe phase, with cracks in this phase which are sites for additional surface area and corrosion.

CONTENTS

FIGURES

TABLES

ACRONYMS

FCRD	DOE Fuel Cycle Research and Development Program
SEM	Scanning Electron Microscopy
EDS	Energy Dispersive X-ray Emission Spectroscopy
BSE	Backscattered Electron
SS	Stainless Steel (Unspecified)
UDS	Undissolved Solids
YSZ	Y_2O_3 Stabilized ZrO_2
Zr	Zirconium
U	Uranium
DU	Depleted Uranium
AWF	Alloy Waste Form
TRUEX	Transuranic Extraction Process
NIST	National Institute of Standards
316SS	Type 316 Stainless Steel
HT9	A type of ferritic steel
RAW	Reference Alloy Waste form
EBR-II	Experimental Breeder Reactor II
M	Molar
DI	Deionized
FY12	Fiscal Year 2012
°C	Degree Celsius
scfh	Standard cubic foot per hour
NMFP	noble metal fission product
x	magnification
FCCI	fuel cladding chemical interaction
RAW-6	Alloy surrogate waste form made in FY16 based on default Ni/Cr concentrations
RAW-6(Ni1)	Alloy surrogate waste form made in FY16 with 1% Ni and 3% Cr added (mass)
RAW-6(Ni3)	Alloy surrogate waste form made in FY16 with 3% Ni and 2% Cr added (mass)
RAW-6(Ni5)	Alloy surrogate waste form made in FY16 with 5% Ni and 1% Cr added (mass)
PEIS	Potentiostatic electrochemical impedance spectroscopy

DURABILITY AND DEGRADATION OF HT9 BASED ALLOY WASTE FORMS WITH VARIABLE NI AND CR CONTENT

1.   INTRODUCTION
1.1   Background

Iron-based alloy waste forms are being investigated to immobilize metallic radioactive species expected from electrochemical treatment methods, such as the undissolved solids (UDS) remaining in the anode basket of the electrorefiner. For conventional sodium cooled fast reactors with metallic fuel and operating in a closed nuclear fuel cycle, these species likely will consist primarily of the alloy fuel cladding, and metals not dissolved in the electrorefiner, primarily Zr, undissolved U diffused into the Zr or cladding, and other trace metals. Similar species are expected from aqueous recycling schemes for used fuel reprocessing, and the iron-based waste form is adaptable to those waste streams.

Prototype waste forms are being formulated and tested to evaluate the capacity to accommodate the radionuclides present in waste streams in durable host phases. Previous work under the Waste Form Campaign has shown U and transuranics to be immobilized in Zr-Fe intermetallic phases, and formulation of the waste form for EBR-II wastes was established to accommodate these radionuclides. The multiple phases in the waste forms can be expected to have different corrosion behaviors and to affect each other's corrosion rates due to electrical coupling under a shared chemical environment. It is important to characterize the effects on corrosion of electrically coupled phases in the multiphase waste form to better predict waste form degradation and waste form release rates or environmental source terms.

A series of materials collectively referred to as RAW-6 was formulated for use in tests at ANL and SRNL to characterize the corrosion behavior and derive model parameter values for a reference alloy waste form made from HT9 and metallic waste streams containing Tc and actinides such as U (Ebert 2015). FCRD-MRWFD-2016-000511, Test Plan for Materials Representing Alloyed Waste Forms Made with HT9 Cladding, called for SRNL to evaluate how the amounts of added Cr and Ni affect the distributions of waste constituents between the host phases formed and the corrosion behaviors of those phases and the overall waste from (Ebert 2015).

1.2   Present Work

This report documents activities that included electrochemical testing, SEM/EDS characterization and leachate sampling the constitutes an accelerated corrosion test protocol that provides information to correlate the electrochemical corrosion test results and release rates from the alloy waste form under accelerated test conditions to the leach rates of specific elements from the alloy waste form under long-term immersion conditions of a repository. Three alloys were characterized, based on the RAW-6 formulations that varied in their Ni and Cr concentration. RAW-6 formulations were determined in FY16 at ANL (Ebert 2015) and the formulations studied at SRNL were also fabricated at SRNL in FY16. RAW-6 represents waste forms made with HT9 steel and surrogate wastes. The purpose of the tests with RAW-6 was to determine parameters for an analytical oxidative-dissolution model and to what extent trim additions of Ni and Cr could be added to improve the corrosion resistance of HT9-based waste forms and compare to ones that used 316SS.

Previous work had shown RAW made with 316 SS to be very corrosion resistant. The added Ni will report to a Zr-Fe phase in the alloy forms that hosts the actinides (e.g. U), whereas the Cr will generally report to an Fe-rich(Fe-Cr) phase that in previous studies was found to host the Re (or Tc surrogate). The EDS data in this report appears to indicate more Re reporting to the $ZrFe_2$ phase than the Fe-rich phase, but this is believed to be primarily from the limited number of EDS points averaged to get the values shown in the table as well as the low accuracy of EDS at small concentrations.

In this report the evaluated alloys are referred to using the added trim mass percent of Ni in the alloy.

This report meets milestone M3FT-17SR030105121, *Issue status report summarizing characterization of microstructures and corrosion behaviors of RAW3 (Ni) materials*, for work package # FT-17SR03010512.

2.   EXPERIMENTAL
2.1   Materials
The materials used for alloy fabrication were high purity. Procedures used for fabricating them were the same as those reported in earlier work (Olson 2012). The chemicals used to make solutions for electrochemical testing were high purity, and the water used for the solutions was demineralized.

2.2   Electrode Chemistry and Phase Distribution Data

Select relevant data on the composition of the electrodes used in this work was compiled and is listed. This data is of use for analyzing the electrochemical data.

Four alloys based on RAW-6 formulation studies were examined by SEM and EDS, three of the alloys were machined into electrodes. Their formulation and averaged elemental make up can be found in Table 1 and Table 2 respectively. The alloys have an added Ni:Cr ratio of 0:0, 1:3, 3:2, and 5:1.

Table 1 HT9 bearing AWF test matrix measured mass additions.

Reagent Mass (g)										
Name	**HT9**	**Zr**	**Mo**	**Ru**	**Pd**	**Re**	**Rh**	**Sn**	**Ni**	**Cr**
RAW-6	7.137	2.254	0.172	0.163	0.122	0.091	0.056	0.006	0.000	0.000
RAW-6(Ni1)	6.966	2.076	0.159	0.151	0.113	0.084	0.052	0.006	0.097	0.289
RAW-6(Ni3)	6.928	2.041	0.156	0.148	0.111	0.082	0.051	0.006	0.295	0.191
RAW-6(Ni5)	6.895	1.996	0.153	0.145	0.109	0.081	0.050	0.006	0.466	0.094

Table 2 HT9 bearing AWF test matrix compositions, present in the alloys above 0.1% by mass or atom, including those of the HT9. Due to rounding, some elements may not show up in all measurement units.

Name	Cr	Mn	Fe	Ni	Mo	Si	W	V	C	Zr	Ru	Pd	Re	Rh	Sn	Cu	Co
Mass Percent																	
RAW-6	8.7	0.3	60.1	0.4	2.5	0.2	0.4	0.2	0.1	22.5	1.6	1.2	0.9	0.6	0.1	0.1	0.1
RAW-6(Ni1)	11.2	0.3	57.8	1.4	2.4	0.2	0.3	0.2	0.1	21.7	1.6	1.2	0.9	0.5	0.1	0.1	0.1
RAW-6(Ni3)	10.2	0.3	57.2	3.3	2.4	0.2	0.3	0.2	0.1	21.4	1.6	1.2	0.9	0.5	0.1	0.1	0.1
RAW-6(Ni5)	9.1	0.3	56.7	5.1	2.4	0.2	0.3	0.2	0.1	21.2	1.5	1.2	0.9	0.5	0.1	0.1	0.1
Atomic Percent																	
RAW-6	6.7	0.2	49.6	0.4	3.5	0.1	1.0	0.2	0.0	30.4	2.4	1.9	2.5	0.9	0.1	0.1	0.1
RAW-6(Ni1)	8.7	0.2	48.0	1.2	3.4	0.1	0.9	0.2	0.0	29.4	2.4	1.9	2.4	0.8	0.1	0.1	0.1
RAW-6(Ni3)	7.9	0.2	47.6	2.9	3.4	0.1	0.9	0.2	0.0	29.2	2.3	1.8	2.4	0.8	0.1	0.1	0.1
RAW-6(Ni5)	7.1	0.2	47.2	4.5	3.4	0.1	0.9	0.2	0.0	28.9	2.3	1.8	2.4	0.8	0.1	0.1	0.1

Two regions are present in the alloys that will be referred to as phases in this report, although they may more accurately be thought of as composition regions. The predominant phases are shown in Figure 1, and their corresponding elemental compositions described in Table 3 and Table 4. The phases are similar to those found in previous work with HT9 based waste forms, and extensive discussion of the characteristic phases in HT9 based waste forms can be found in the report Formulation of Reference Alloy Waste Form RAW-3, and only a brief discussion is included here (Olson 2012).
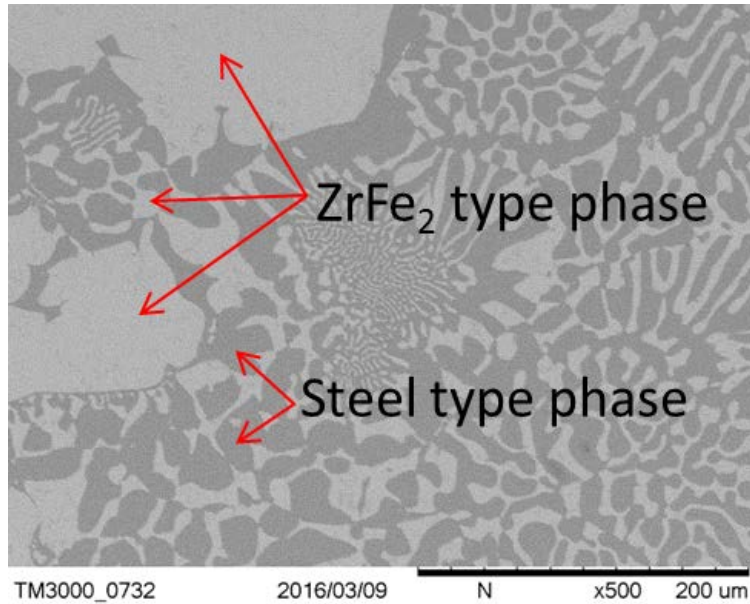
Figure 1. RAW-6(Ni3) alloy showing two dominant phases.

In Table 3 and shown in Figure 1, the dark regions represent a steel phase assumed to be ferrite based on previous XRD characterization of the bulk alloy, and the phase assemblage characteristics of HT9 alloy. When Cr is added to the alloy, this region has higher Cr concentrations, and when Ni is added higher Ni concentrations are observed. If trends observed in previous HT9 based alloys holds for this composition, this phase represents the area to where the

majority of the Tc in any waste form will segregate. The EDS data in this report appears to indicate more Re reporting to the $ZrFe_2$ type phase than the Steel type phase, that is inconsistent with previous results. However, this present observation has high uncertainty due to the limited number of EDS points averaged to get the values shown in the table as well as the limited capability of EDS to provide an accurate concentration at small concentrations of species in a phase.

Table 3 EDS point scans of apparent similar composition ranges corresponding to the steel type phase composition in Figure 1, and corresponding compositions in the other alloys. This region is believed to correspond to ferrite due to the low Ni and high Cr content.

Steel Type Phase (atomic %)													
Name	Si	V	Cr	Mn	Fe	Ni	Zr	Mo	Ru	Rh	Pd	Sn	W	Re
RAW-6	0.1	0.6	15.9	0.9	80.4	0.3	0.1	1.5	0.2	0.0	0.0	0.0	0.1	0.0
RAW-6(Ni1)	0.2	0.5	20.4	0.4	76.3	0.2	0.1	1.5	0.1	0.2	0.0	0.1	0.0	0.0
RAW-6(Ni3)	0.5	0.4	19.5	0.1	76.3	1.2	0.2	1.5	0.3	0.0	0.0	0.0	0.1	0.0
RAW-6(Ni5)	0.0	0.3	16.7	0.5	77.6	2.8	0.2	1.5	0.1	0.1	0.0	0.1	0.0	0.2

Table 4 and shown in Figure 1 is the composition range for the phase assumed to be the $ZrFe_2$ type phase. This is based on previous from EBR-II waste form research. This is the predominant phase in the both the 316SS-based and HT9-based alloys where actinides report. In the EBR-II waste forms the U-rich $ZrFe_2$ type (Laves type) phases usually had no less than ~40 at% Fe, ~12.5-25.7 at% Ni, and Zr and U concentrations adding to ~25-30 at% (Keiser 2000), which closely resembles the regions shown in Figure 1 and Table 4. The lower Ni content in the RAW6 alloys than that reported in literature is due to the low Ni content of the HT9 alloy used to make the present alloys, whereas higher Ni content alloys were used in previous studies.

Table 4 EDS point scans of apparent similar composition ranges corresponding to the $ZrFe_2$ composition in Figure 1, and corresponding compositions in the other alloys.

$ZrFe_2$ Type Phase (atomic %)													
Name	Si	V	Cr	Mn	Fe	Ni	Zr	Mo	Ru	Rh	Pd	Sn	W	Re
RAW-6	0.3	0.4	5.8	1.1	65.1	0.4	22.1	1.4	1.0	0.3	1.5	0.1	0.2	0.2
RAW-6(Ni1)	0.6	0.0	7.4	0.8	60.4	1.5	24.0	1.7	1.5	0.8	1.2	0.0	0.2	0.1
RAW-6(Ni3)	0.5	0.1	6.2	0.2	60.5	5.7	22.4	1.4	1.2	0.5	0.6	0.0	0.1	0.6
RAW-6(Ni5)	0.7	0.2	4.5	0.7	57.1	8.4	23.5	1.4	1.3	0.7	0.9	0.1	0.2	0.2

The data in Table 5 is of direct use for performing calculations with the electrochemical data from the Bare Surface (fresh grind/polish of the surface) measurements as well as the hybrid electrochemical/immersion testing; such as analyzing the potentiodynamic data and determining the current density. Each of the RAW formulations was made into an electrode, but only the RAW-6(Ni1), RAW-6(Ni3), and RAW-6(Ni5) electrodes were used for bare surface characterizations.

After the bare surface characterizations, characterization of the long term evolution of the passivation film focused on the RAW-6(Ni3) electrode and two additional electrodes were made from this alloy to allow for multiple hold potentials to be examined in different solutions

simultaneously for this alloy. The electrode surface areas were kept constant by attaching an insulated wire to the alloys, then embedding the alloys in EpoFix nonconductive epoxy, prior to electrode surface preparation.

Table 5 Electrode density, equivalent weight, and Surface area of the alloys for the bare surface potentiodynamic scans.

Designation	Density (g/cm^3)	Equivalent Weight	Surface area^A (cm^2)
RAW-6	7.8	25.1	0.87
RAW-6(Ni1)	7.8	24.8	0.88
RAW-6(Ni3)	7.9	25.0	0.95
RAW-6(Ni5)	7.9	25.1	0.98

A) Bare surface Potentiodynamic Scan

The electrodes were reground, polished, and their refreshed surface areas measured for each of the hybrid tests to achieve more consistent monitoring of the passivation process of the surfaces and because the hybrid testing was potentially more aggressive to the electrode surfaces and therefore previous tests could influence later tests if specific phases were selectively attacked and the surfaces were not brought back to as standard initial state. The electrode that was used for the 300 mV (vs. SCE) potentiostatic hold suffered from severe (deep) localized corrosion attack and it was not practical for reuse.

Table 6 Electrode surface areas prior to hybrid testing for the RAW-6(Ni3) electrode.

Hold Potential (vs. SCE)	Surface area (cm^2)
-100	1.02
0	1.00
100	1.06
200	1.08
300	1.05
E_{Corr} A	1.00
E_{Corr} B	1.06

Figure 2 and Figure 3 show the microstructure of the as fabricated pre-exposure multiphase alloys used for the SEM and EDS analysis and for the electrochemical and hybrid testing.

Durability and Degradation of HT9 Based Alloy Waste Forms with Variable Ni and Cr Content
FCRD-MRWFD-2017-000407
SRNL-STI-2016-00719
December 31, 2016

14
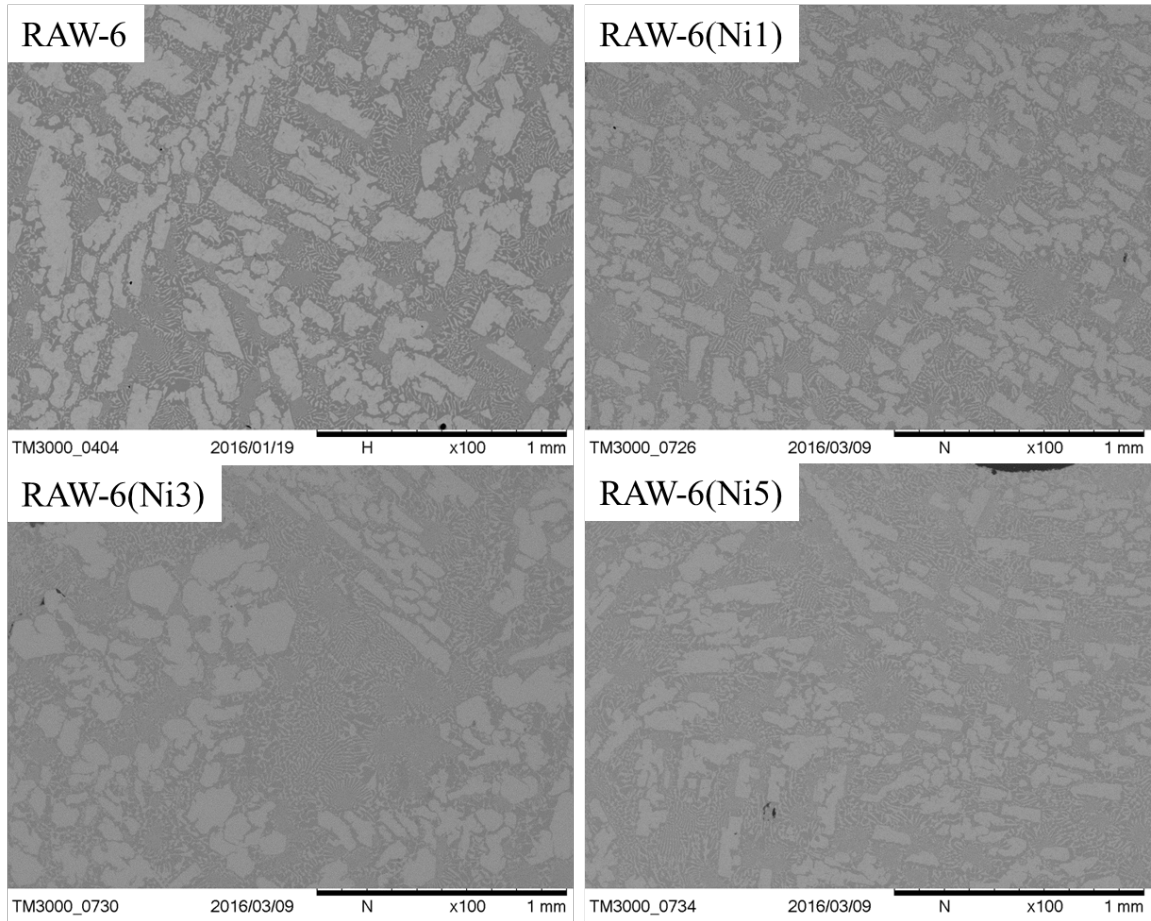
Figure 2 Low magnification SEM showing characteristic morphologies of the fabricated alloys for RAW-6 Ni and Cr trim addition studies.
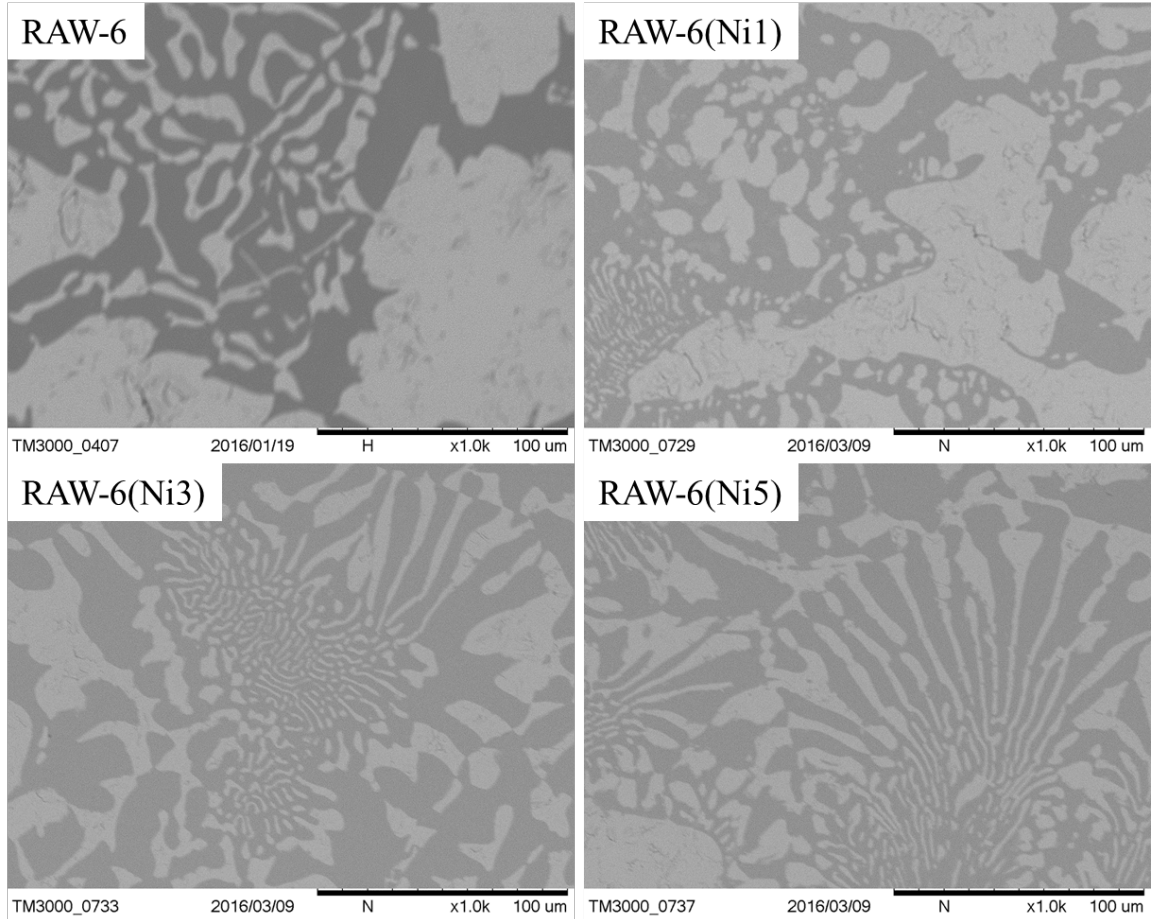
Figure 3 Higher magnification SEM showing characteristic morphologies of the fabricated alloys for RAW-6 Ni and Cr trim addition studies.

SEM images at magnification of 100x and 500x were analyzed using the ImageJ program to ascertain any clear changes in the contribution of specific phases with changing alloy elemental make-up. No clear trends in phase areal fraction were found to be functions of either Cr or Ni that held for both high and low magnification images.

Table 7 Phase areal concentration for each alloy.

			Area fraction (%)			
	atomic %		low mag (100x)		High mag (500x)	
Designation	Cr	Ni	Fe phase	Zr-Fe phase	Fe phase	Zr-Fe phase
RAW-6	10.5	0.5	43.4	56.6	36.9	63.1
RAW-6(Ni1)	13.6	1.5	47.3	52.7	54.5	45.5
RAW-6(Ni3)	12.4	3.6	48.7	51.3	40.1	59.9
RAW-6(Ni5)	11.2	5.4	49.2	50.8	46.6	53.4

2.3   Electrochemistry Parameters

Specific test parameters can be found in APPENDIX 1: Electrochemical Measurement Data.

2.3.1   Test Cells and Solution Preparation

The electrochemical testing was undertaken in Greene cells that held 700 mL of solution that was de-aerated using argon gas. The solutions used were alkaline or acidic brines titrated to pH values of 3, 5, 8, and 10 with dilute solutions of NaOH or H_2SO_4. The alkaline and acidic brines used to initially fill the cells prior to titration were according to the Electrochemical Testing Protocol. The Electrochemical Testing Protocol was developed collaboratively by multiple laboratories working in the area of alloy waste form corrosion:

$$\frac{0.1 \text{ mmol NaOH} + 10 \text{ mmol NaCl}}{1 \text{ kg } H_2O}$$

And

$$\frac{0.1 \text{ mmol } H_2SO_4 + 10 \text{ mmol NaCl}}{1 \text{ kg } H_2O}$$
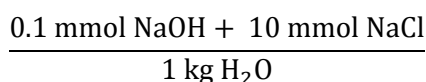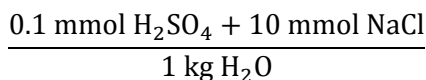
To make each Greene cell solution, a concentrated 100x strength solution was made, then diluted with demineralized water. The freshly mixed solution was deaerated by sparging with argon for 30 min, then titrated to the desired pH, then sparged for 1 hour after which the pH was verified to be at the desired value, and adjusted if necessary.   The solution temperatures varied with ambient temperatures, with recorded values varying from 20-22 °C.

2.3.2   Bare Surface Measurements

Bare Surface tests were performed on RAW-6(Ni1), RAW-6(Ni3), and RAW-6(Ni5). The Bare Surface tests first involved an open circuit potential measurement for 60 seconds to allow the system to settle and the electrodes underwent a potentiodynamic scan from   -500 mV to 1000 mV (vs. SCE). After each set of Bare surface measurements at a particular pH, the electrodes were repolished for the next set of measurements at the new pH. Following testing, the electrodes were examined via SEM/EDS.

2.3.3   Hybrid Testing

The hybrid tests utilized electrodes made from RAW-6(Ni3), and involved long-term exposures (up to 7 days) coupled with electrochemical testing consisting of potentiostatic holds and with potentiostatic electrochemical impedance spectroscopy (PEIS) at selected exposure times. The test would start with an open circuit measurement of about 1 minute, followed by a cleaning potential hold at -500 mV for about 2 minutes, and be followed by a trial potential hold at the test potential for about 2 minutes, prior to the hybrid test starting in full. The primary hybrid testing involved potentiostatic holds that would last for 20 hours, after which the PEIS would occur at about the same potential, with this pattern repeated for 7 days. Solution samples would be taken at about 1, 2, 4, and 7 days of exposure, preferably during the potentiostatic hold. For these tests, only the RAW-6(Ni3) alloy was investigated, but three electrodes were made from this alloy for

testing. The electrodes started the tests in a polished condition, and then underwent the following protocol:

- Gamry acquisition program (tests occurred in order from 1 to 5)

    1. Open Circuit Potential (OCP) measurement for 60 sec

    2. Potentiostatic Hold (PS) at V= -500 mV vs. SCE for 120 sec (reductive cleaning)

    3. PS at V=V1 vs. SCE for 120 sec (V1 is the selected test voltage)

    4. Loop (repeat 7 times):

        a. PEIS at V=V1 vs. SCE

        b. PS at V=V1 vs. SCE for 20 hr

    5. PS at V=V1 vs. SCE until test terminated and electrode removed. The time for this step was set for 24 hours, but the electrode was removed during this step.

- After the electrochemical tests, the electrode surfaces were examined via SEM/EDS, looking for attacked phases from the potentiostatic hold.

- The electrodes were then repolished for subsequent tests and the repolished surfaces were examined by SEM to ensure a refreshed surface.

- Aliquot of the Greene cell solutions were taken at hybrid test days 1, 2, 4, and 7.

2.3.4 E_{Corr} Evolution

The E_{Corr} measurements were performed in duplicate with the RAW-6(Ni3) electrodes. PS hold measurements were undertaken in which the potential was fixed and the current measured and recorded for several different potentials. It was suspected that the current would quickly settle at some potential, with the lowest potential that the current settled at being close to the near steady state corrosion potential. To find the E_{Corr}, first the OCP was measured for 60 seconds, then a PS hold for 1 hour at -450 mV vs SCE was made, then the PS hold potential was moved in +50 mV increments of 1 hour long PS holds with the final PS hold at 150 mV vs SCE.

2.3.5   Individual Electrochemical Measurement Parameters

The following individual electrochemical measurement parameters were used:

Open Circuit Potential (Used at the beginning of all electrochemical tests)
    Time per point (s): 1
    Duration (s): 60s when used just before measurements
    Drift Rate (mV/min): 0

Potentiostatic hold (Used for Hybrid testing and E_{Corr} Evolution tests)
    Potential (V): At the test potential which varied in tests from -150 mV to 300 mV vs SCE (RHE used in tests)
    Time per point (s): 10
    Duration (s): ~20 hours (sometimes repeated)

Potentiostatic EIS (Used for Hybrid testing)
AC Properties
Start Freq (Hz): 100 000
End Freq (Hz): 0.001
Amplitude (mV RMS): 10
DC Properties
Step or Scan Potential (V): Step=0, At Potentiostatic hold potential for those measurements
Scan Properties
Points per Decade: 10
Data Quality: 1
Measurements Delay (s): 0

Potentiodynamic (Used for Bare Surface Characterizations)
Initial Potential (V): -0.500 vs SCE
Final Potential (V): 1.0 vs SCE
Sweep rate (mV/s): 0.167
Current limit (mA): 10

2.4   Analytical Equipment

SEM and EDS Analysis
A Hitachi TM3000 SEM with a Bruker Quanta 70 x-ray acquisition system was used for pre and post exposure morphological examination. The SEM images utilized a backscattered electron (BSE) detector. The accelerating voltage used for the BSE and EDS analyses was 15 kV.

Mass Measurements
The mass of the alloy waste form components, crucibles, and all other pertinent mass information, was measured on a Sartorius CP324S analytical balance.

Gamry Potentiostats
Electrochemical measurements were made with Gamry Reference 600 Potentiostats controlled with Gamry software. Electrochemical data was analyzed using Microsoft Excel and CorrView software.

3.   RESULTS AND DISCUSSION

Three alloys based on the RAW-6 formulation, with 3 different concentrations of Ni and Cr, were characterized with electrochemical measurements. The electrochemical measurements included bare surface characterizations and hybrid tests. The bare surface characterizations involved running a potentiodynamic scan at a select pH on a freshly polished electrode surface. The hybrid tests consisted of potentiostatic holds of up to 1 week while exposing the alloys to corrosive conditions. Simultaneously to the electrochemical measurements for they hybrid testing, solution samples were pulled periodically and measurements were taken to correlate to the electrochemical data. Post exposure/monitoring select electrodes were characterized via SEM.

3.1   Bare Surface Potentiodynamic Measurements

Potentiodynamic measurements were taken on freshly polished electrodes in acidic and alkaline brines, nominal pH 3 pH 5, pH 8,and pH 10. Figure 4 shows the compilation of all the different

potentiodynamic data for the three electrodes in all 4 pH solutions, and Figure 5, Figure 6, Figure 7, and Figure 8 show the alloy behavior changes with trim metal additions in each of the 4 pH values tested. In all but the most acidic pH 3 solutions, the corrosion current is near -0.40 Volts versus SCE.

In all solutions for all alloys, transpassive behavior begins, as signified by large jumps in current, around 350 mV to 400 mV. This region is believed to be influenced by concentrations of Pd, Ni, Zr, and U. The passive region is believed to be most affected by the addition of Cr, and lies above E_{Corr} and below the transpassive region.
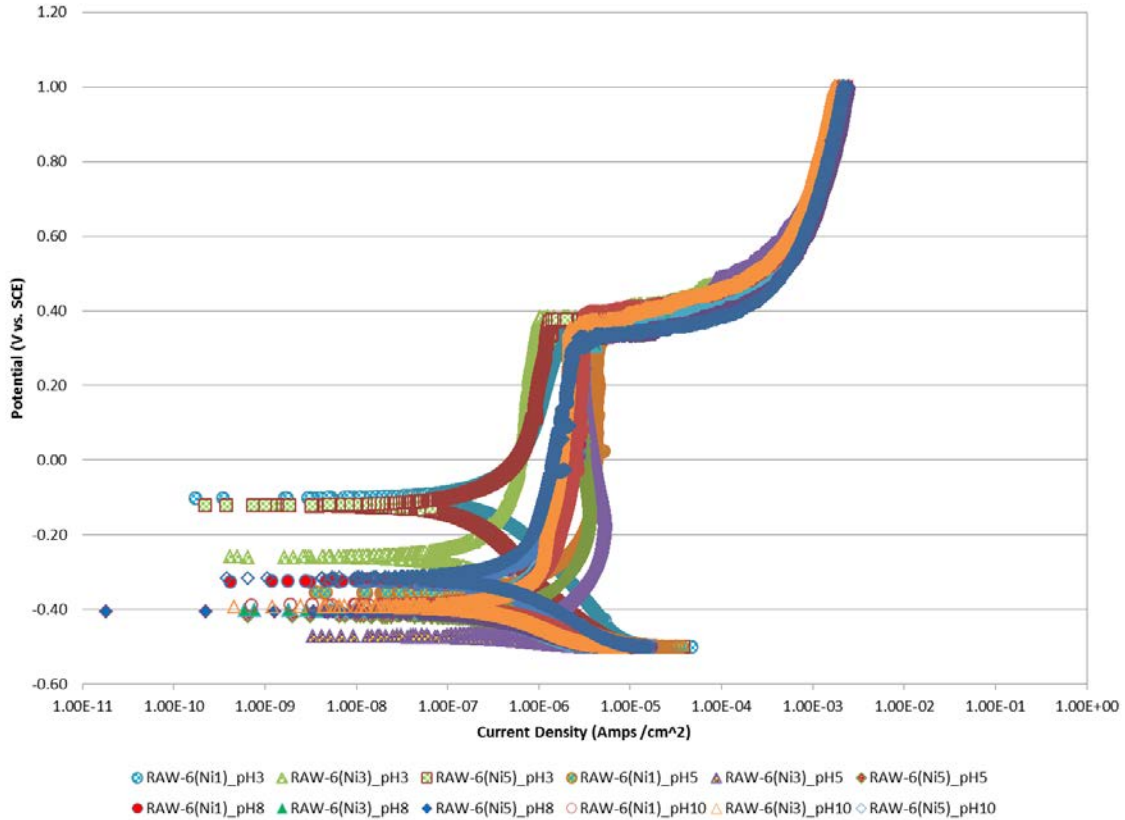
Figure 4 Comparison of Potentiodynamic scans of RAW-6 alloys with fresh polished surfaces in acidic and alkaline brines.
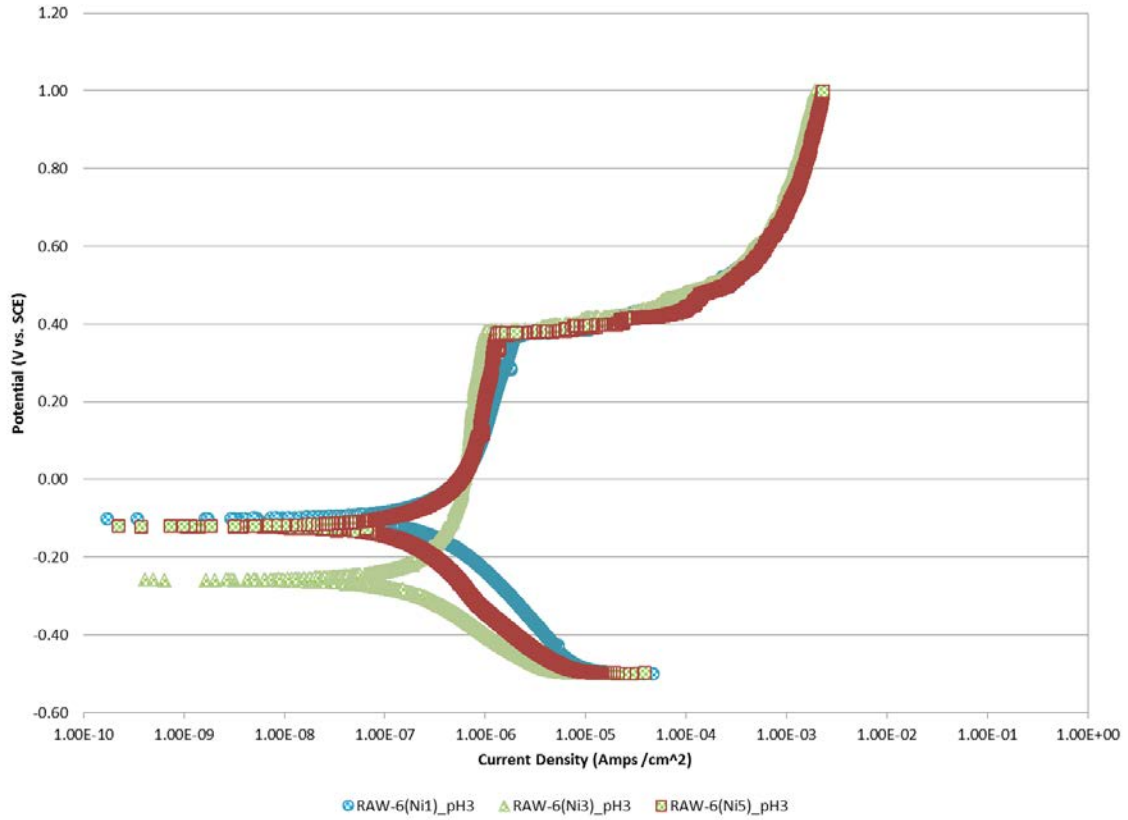
Figure 5 Comparison of Potentiodynamic scans of RAW-6 alloys at pH 3.

Durability and Degradation of HT9 Based Alloy Waste Forms with Variable Ni and Cr Content
FCRD-MRWFD-2017-000407
SRNL-STI-2016-00719
December 31, 2016

21
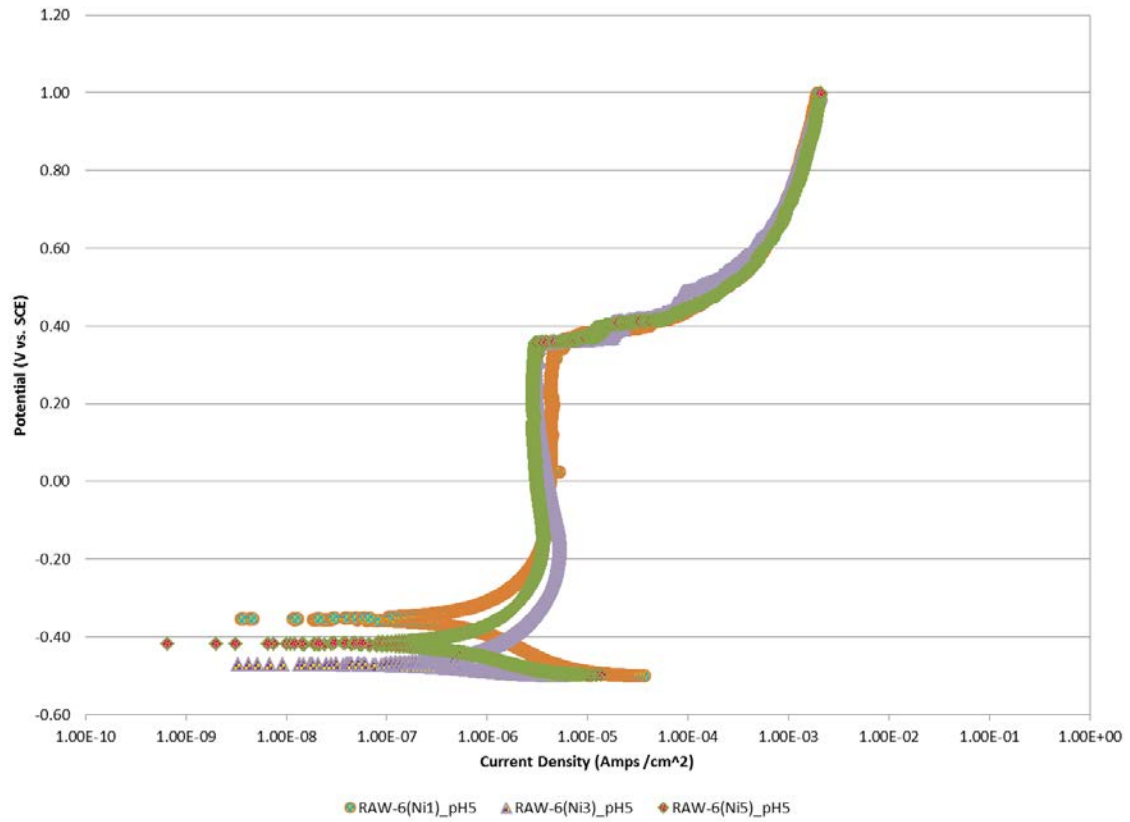
Figure 6 Comparison of Potentiodynamic scans of RAW-6 alloys at pH 5.
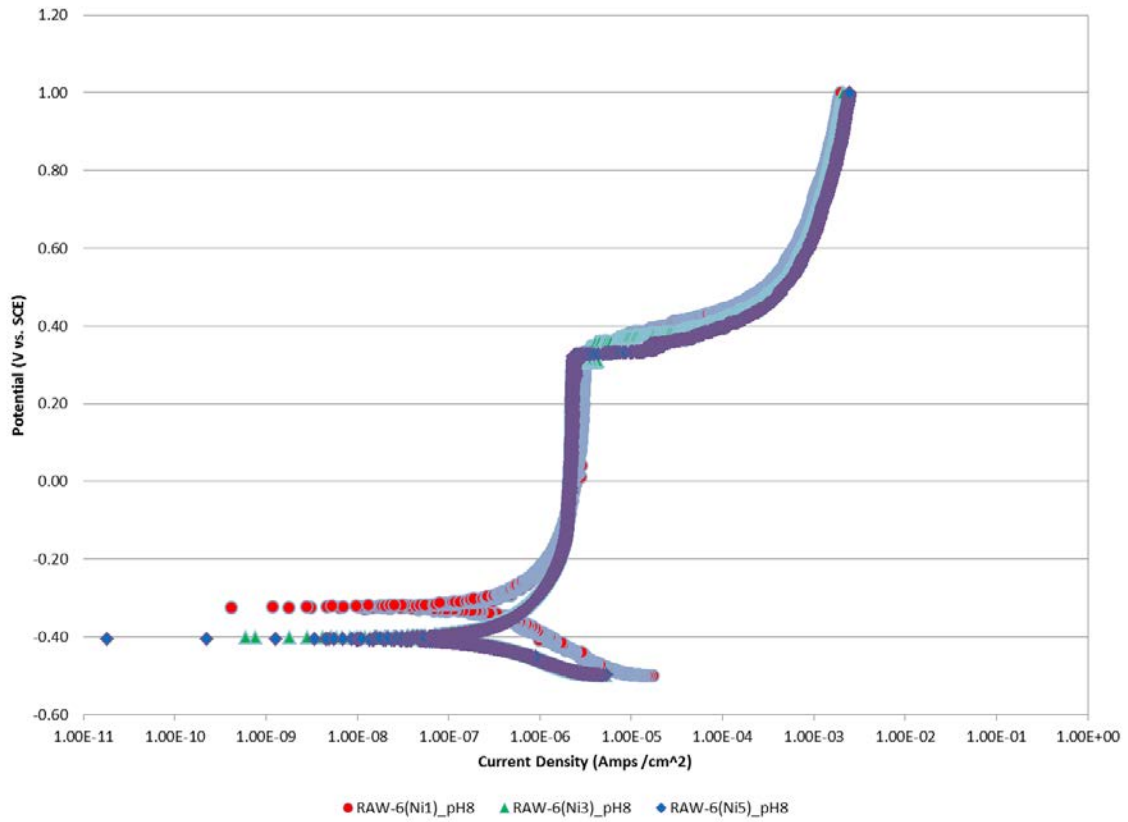
Figure 7 Comparison of Potentiodynamic scans of RAW-6 alloys at pH 8.
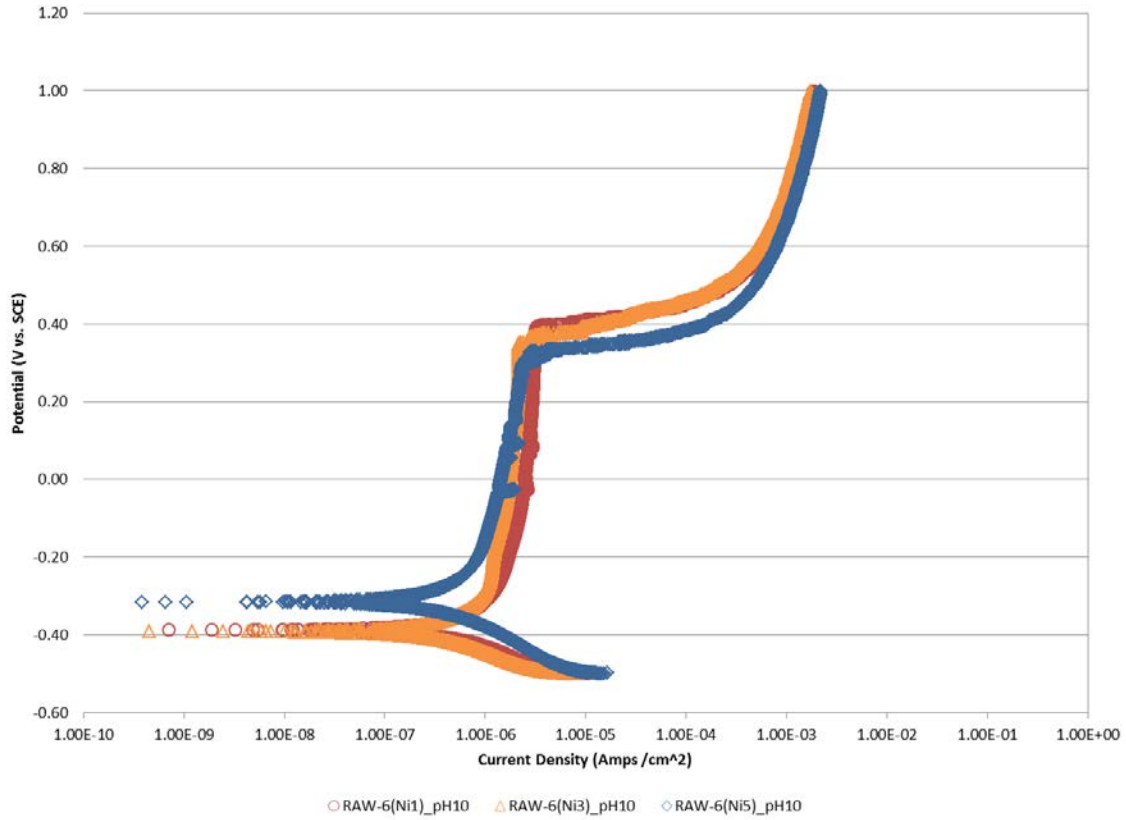
Figure 8 Comparison of Potentiodynamic scans of RAW-6 alloys at pH 10.

Figure 9 compares the current density from the Potentiodynamic scan of the RAW-6(Ni3) alloy in pH 3 solution to the final current densities measured during the hybrid testing for the same alloy and solution. It is observed that the -100 mV potentiostatic hold leads to a reducing surface condition, and the 0 to 200 mV potentiostatic holds lead to a passivated surface and reduced currents. However the 350 mV potentiostatic hold leads to increased currents as the alloy shifts to transpassive behavior.
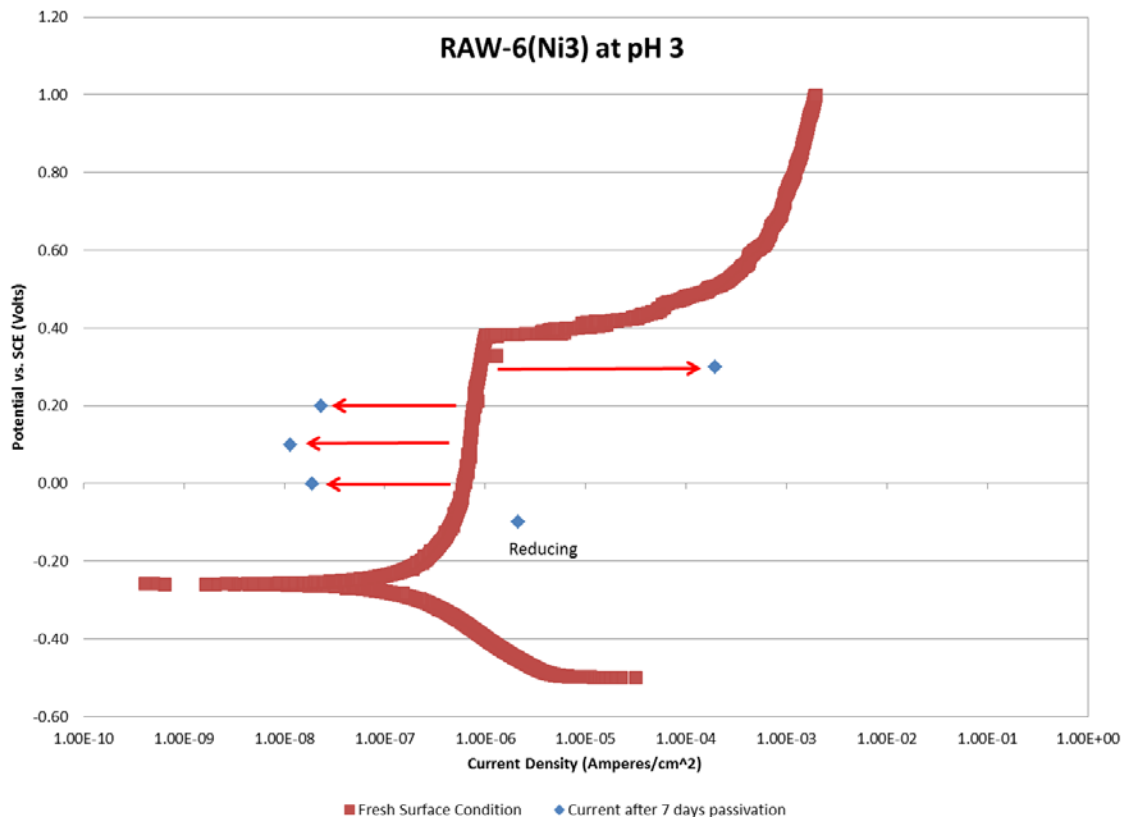
Figure 9 **Comparison of Potentiodynamic scan current density of RAW-6(Ni3) alloy at pH 3 with the final recorded current density after about 7 days of hybrid testing.**

3.2   Hybrid Testing Potentiostatic Corrosion Current Densities

The primary measurement of the hybrid immersion/electrochemical test was the recording of alloy waste form corrosion currents under constant electrode potential. This data was recorded for 5 hybrid tests, and the corrosion currents are summarized in Figure 10, Figure 11, Figure 12, Figure 13, and Figure 14. Note the time in the figures on the x-axis is given in seconds in UNIX time to better correlate events observed electrochemically on the electrode to the solution samples. Furthermore, each individual potentiostatic current recording is labeled for the day and time in which it was initiated. All of the hybrid tests utilized the RAW-6(Ni3) alloy and a acidic brine solution of pH 3, but held the potential at different values.

The -100 mV potentiostatic hold, Figure 10, demonstrated that at this potential value, the electrode surface on average quickly attained a reducing condition. The first potential hold current density shown in Figure 10 starts after about 5 hours and 28 minutes into the potential hold, with earlier data not shown due to the large shifts in current often seen in the first few hours, as well as the data being stored in the PEIS data file. The data in the PEIS data file showed that positive currents were first observed after about 2 minutes of exposure to the -100 mV potential hold, but fluctuated between positive and negative currents until about 1 hour of exposure, after which the current density remained negative (reducing). This indicates that E_{Corr} also shifts positive in potential, at least above -100 mV.

Durability and Degradation of HT9 Based Alloy Waste Forms with Variable Ni and Cr Content
FCRD-MRWFD-2017-000407
SRNL-STI-2016-00719
December 31, 2016

25
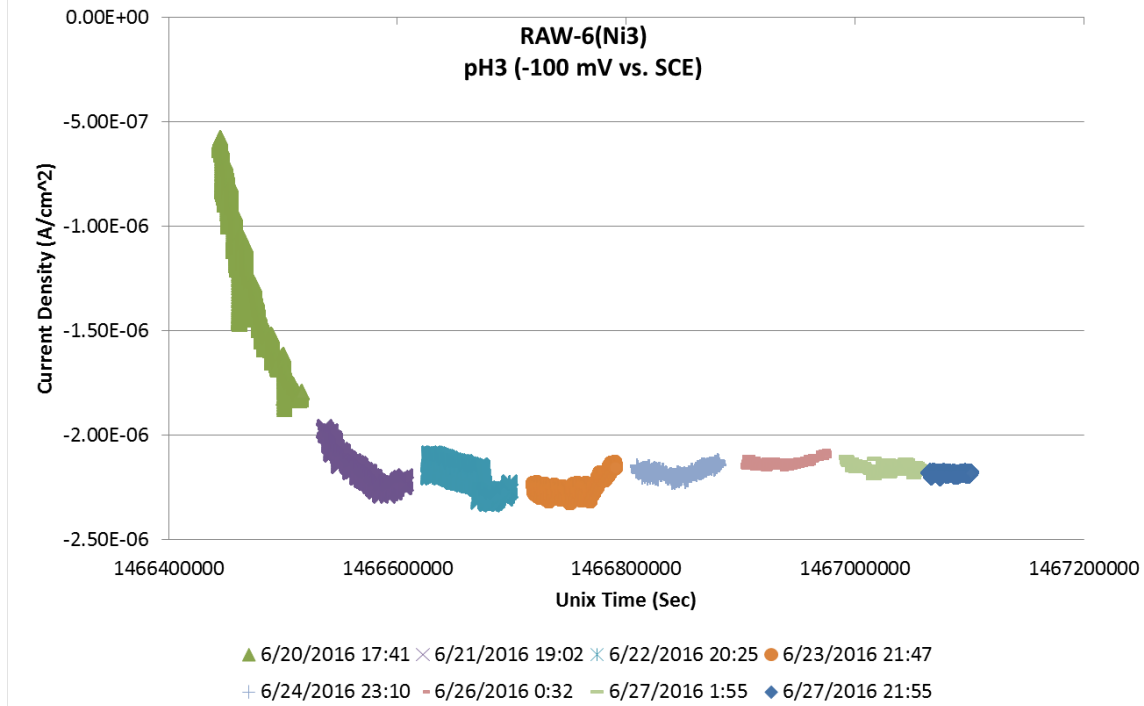
Figure 10 Current compilation with time for the RAW-6(Ni3) electrode held at -100 mV in acidic brine at pH 3. Note the time is given in seconds in UNIX time to better correlate to the time the solution samples were withdrawn. Each individual potentiostatic current recording is labeled for the day and time in which it was initiated.

The 0 mV, 100 mV, and 200 mV potentiostatic holds all showed similar behavior and currents, indicating that at these potential values, the alloy electrode surface remains in the passive region. For these three potentials, the current rapidly drops in the first day, and then gradually decreases throughout the test duration.
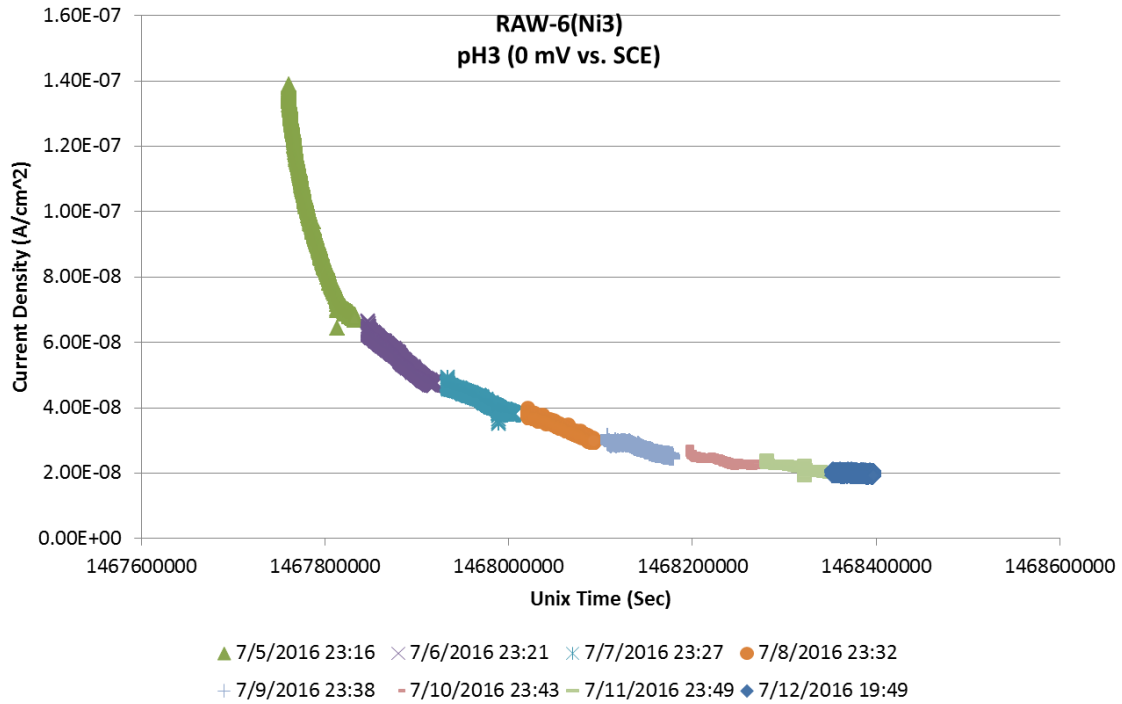
Figure 11 Current compilation with time for the RAW-6(Ni3) electrode held at 0 mV in acidic brine at pH 3. Note the time is given in seconds in UNIX time to better correlate to the time the solution samples were withdrawn. Each individual potentiostatic current recording is labeled for the day and time in which it was initiated.
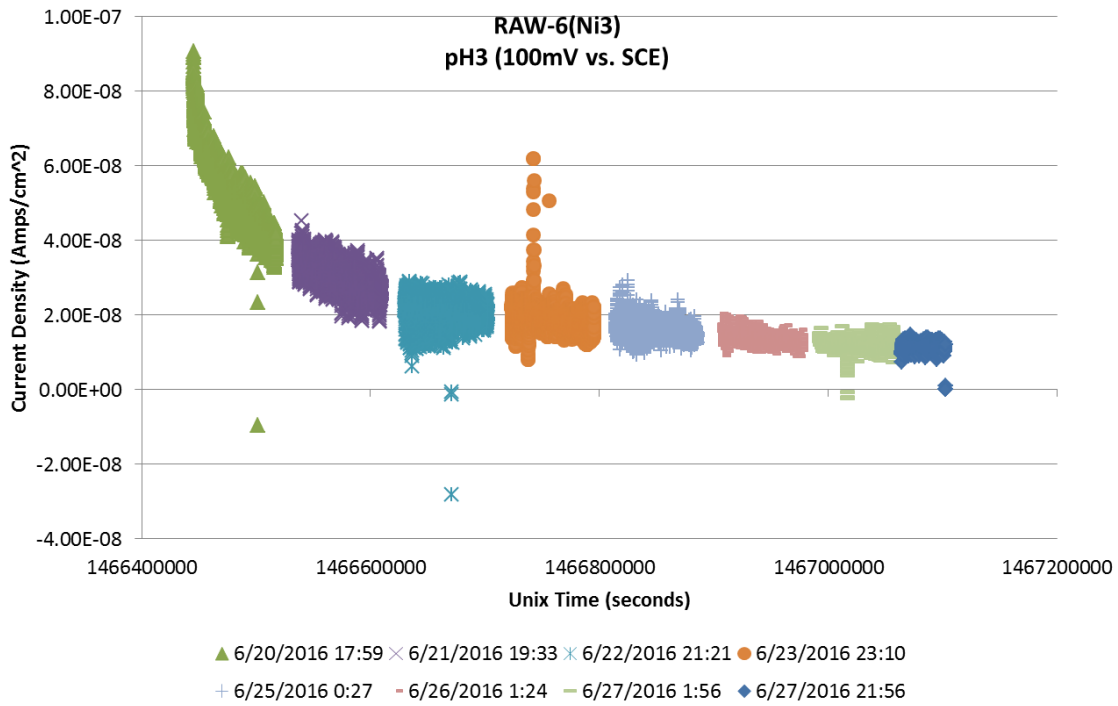
Figure 12 **Current compilation with time for the RAW-6(Ni3) electrode held at 100 mV in acidic brine at pH 3. Note the time is given in seconds in UNIX time to better correlate to the time the solution samples were withdrawn. Each individual potentiostatic current recording is labeled for the day and time in which it was initiated.**
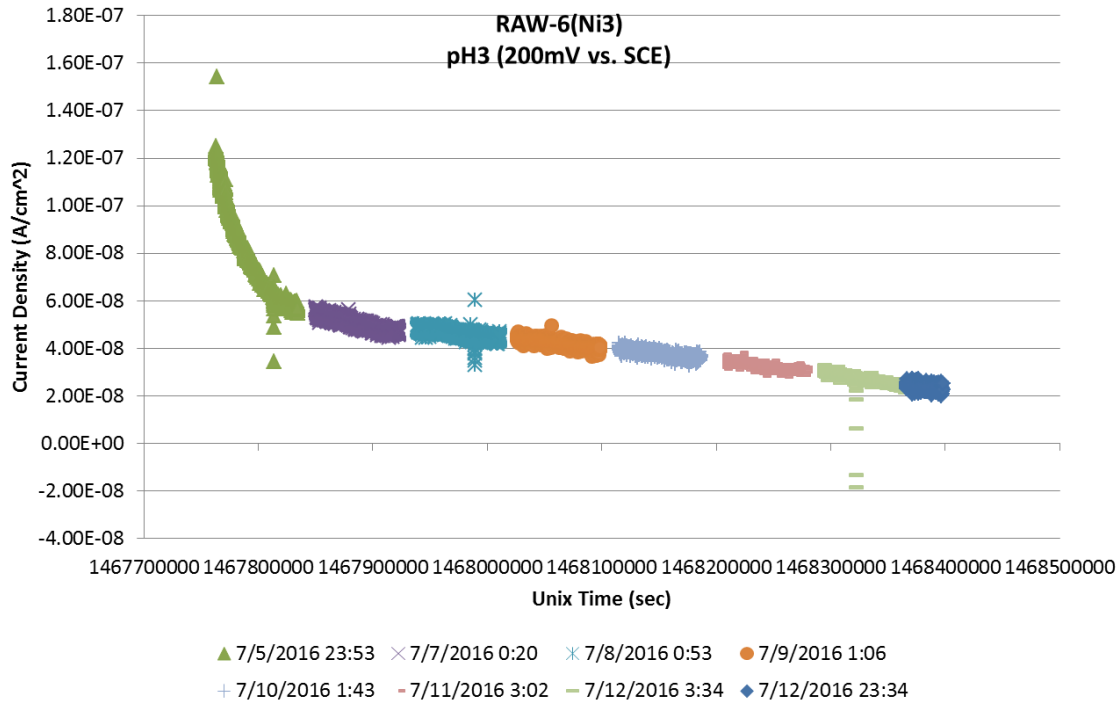
Figure 13 Current compilation with time for the RAW-6(Ni3) electrode held at 200 mV in acidic brine at pH 3. Note the time is given in seconds in UNIX time to better correlate to the time the solution samples were withdrawn. Each individual potentiostatic current recording is labeled for the day and time in which it was initiated.

The 300 mV potential hold current density indicates that the alloy when held at this potential shifts to transpassive behavior. The electrode current increases in a linear fashion.
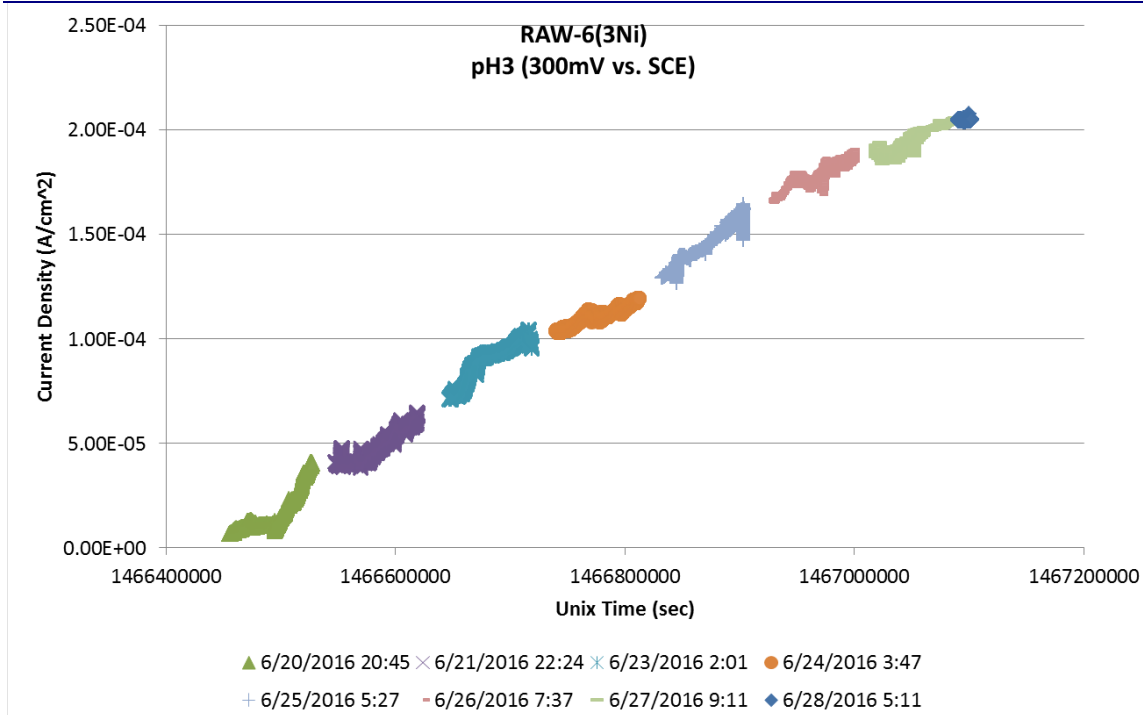
Figure 14 Current compilation with time for the RAW-6(Ni3) electrode held at 300 mV in acidic brine at pH 3. Note the time is given in seconds in UNIX time to better correlate to the time the solution samples were withdrawn. Each individual potentiostatic current recording is labeled for the day and time in which it was initiated.

3.3   Hybrid Testing Potentiostatic Electrochemical Impedance Spectroscopy

The potentiostatic electrochemical impedance spectroscopy (PEIS) data is used to probe the nature of the degradation of the alloy electrode surface and formation of any corrosion product films. The PEIS data is presented as Bode gain plots, Bode phase plots, and Nyquist plots. The PEIS data collectively indicates the -100 mV potentiostatic hold made the alloy electrode surface stable, but without a protective passivation layer. The 0 mV, 100 mV, and 200 mV PEIS data collectively show stable surfaces that appear to become more stable with time. The 300 mV PEIS data shows an unstable surface with no passivation that may become increasingly active with time.

3.3.1   Bode Plots

In the Bode gain plots, Figure 15 through Figure 19, the high frequency region of the curve is heavily influenced by solution resistance and the lower frequency range by the interaction between the electrode and the solution, with the lowest values giving understanding similar to the polarization resistance. The -100 mV potential hold Bode gain plot, Figure 15, drops in value at the low frequency ranges, then maintains relatively constant behavior throughout its frequency range, indicating the electrode surface does not change much in its behavior with the solution after the first day. PEIS and EIS is most useful if performed on stable systems, but unstable data sets are shown here primarily to indicate the unstable nature of the passivation layer. The Bode gain plot of the -300 mV PEIS, Figure 19, shows an unstable surface that is continually changing, and presenting less polarization resistance with time. The 0 mV, 100 mV, and 300 mV Bode

plots, Figure 16, Figure 17, and Figure 18, respectively, all show a very stable surface-solution interaction. At the lowest frequencies, it appears that the 0 mV and 100 mV surface becomes increasingly passive, but the 200 mV surface appears to have reached a maximum resistance, then started to decrease.
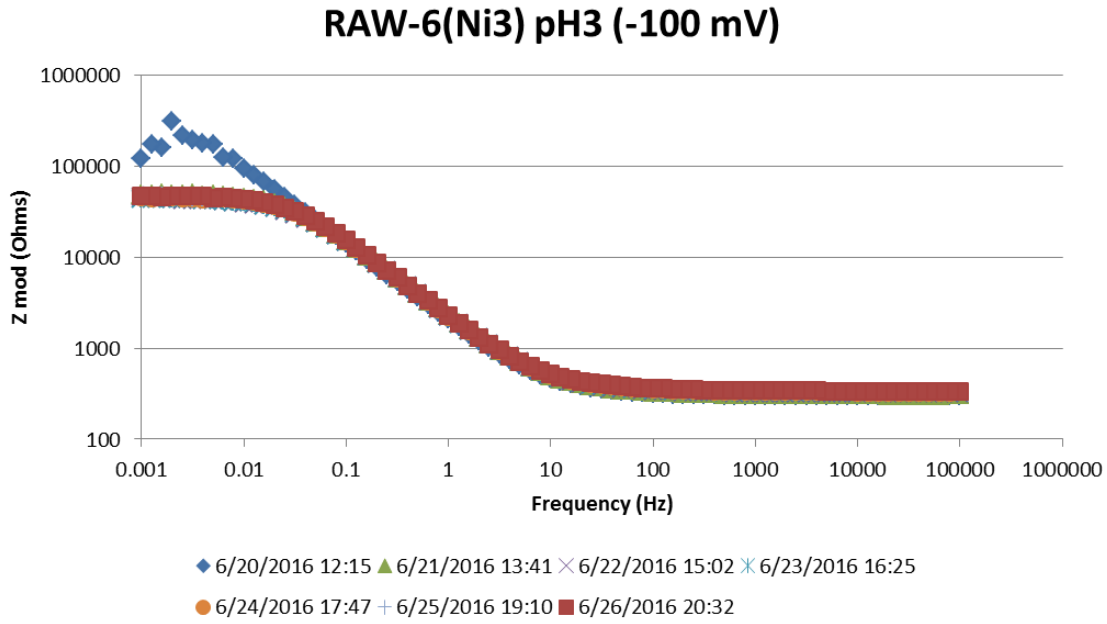
Figure 15 Bode gain plot for -100 mV potentiostatic EIS in alkaline brine for the RAW-6(Ni3) alloy electrode.
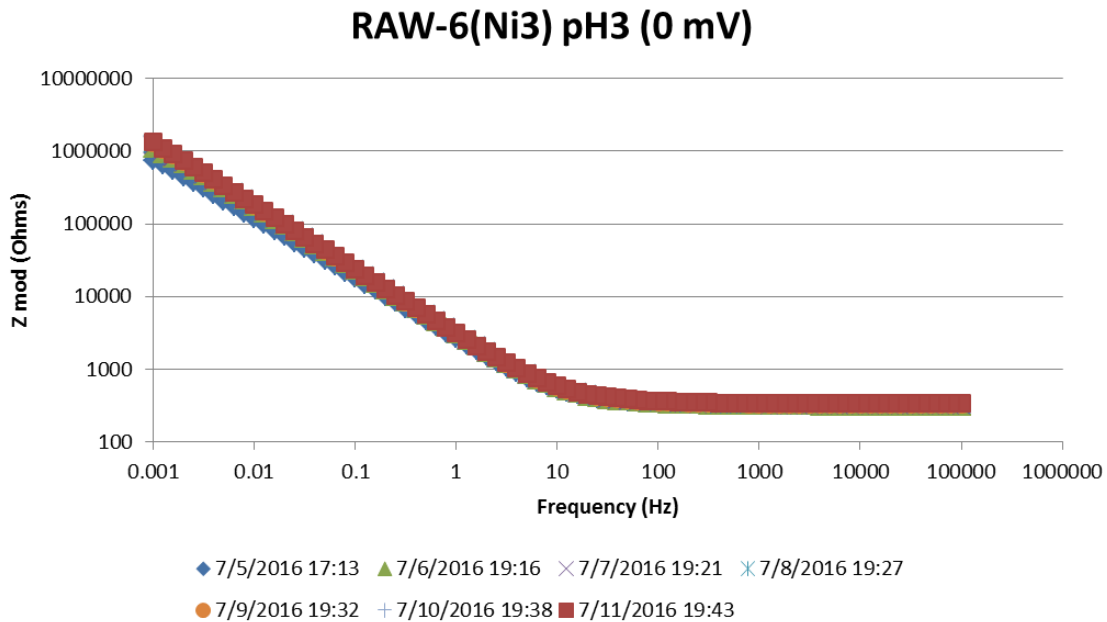
Figure 16 Bode gain plot for 0 mV potentiostatic EIS in alkaline brine for the RAW-6(Ni3) alloy electrode.

Durability and Degradation of HT9 Based Alloy Waste Forms with Variable Ni and Cr Content
FCRD-MRWFD-2017-000407
SRNL-STI-2016-00719
December 31, 2016

31
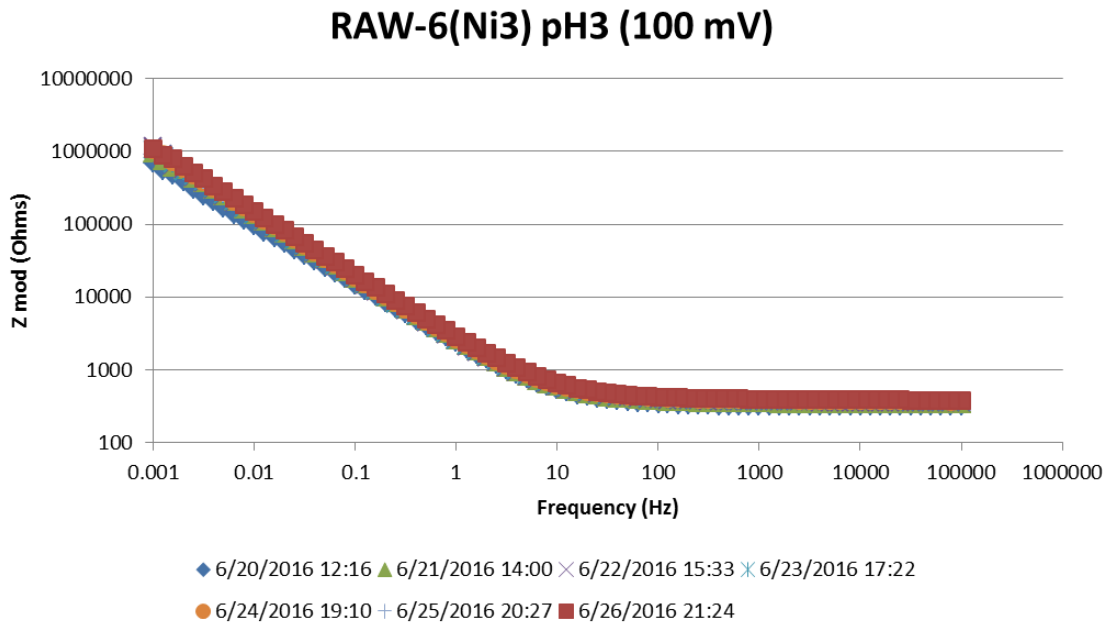
Figure 17 Bode gain plot for 100 mV potentiostatic EIS in alkaline brine for the RAW-6(Ni3) alloy electrode.
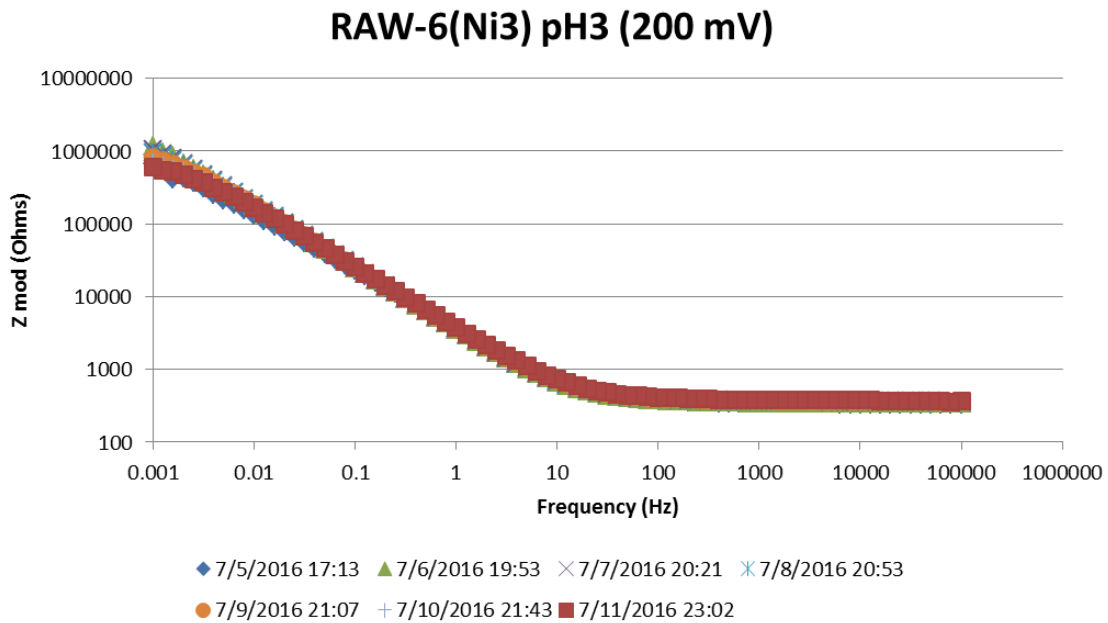
Figure 18 Bode gain plot for 200 mV potentiostatic EIS in alkaline brine for the RAW-6(Ni3) alloy electrode.
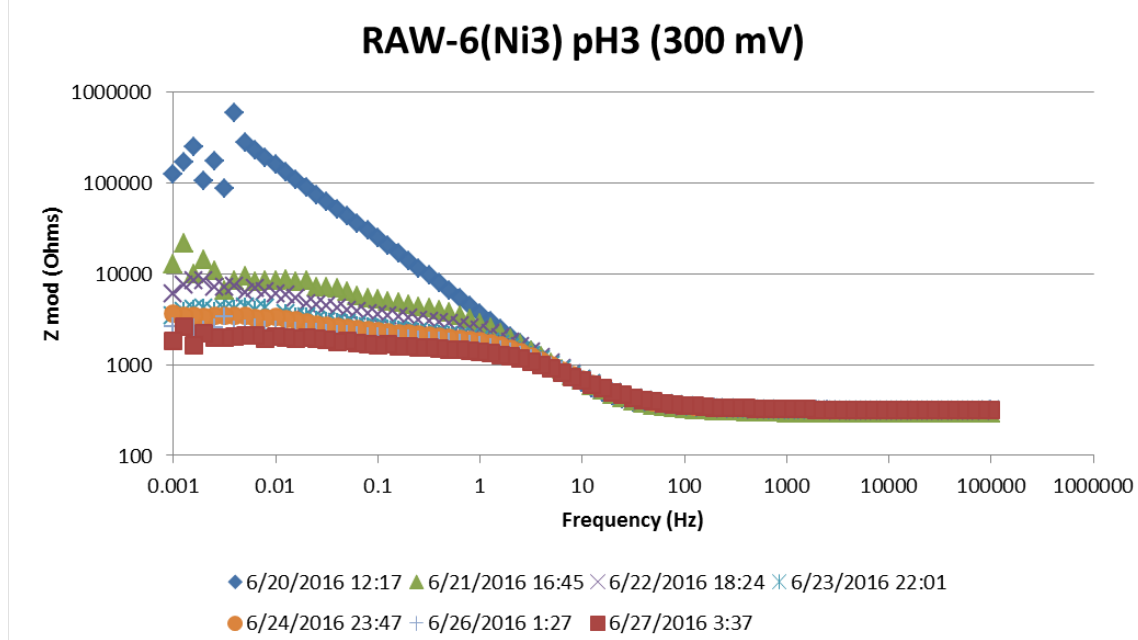
Figure 19 Bode gain plot for 300 mV potentiostatic EIS in alkaline brine for the RAW-6(Ni3) alloy electrode.

The Bode phase plots, Figure 20 through Figure 24, indicate that there are fast and slow events occurring between the electrode surface and the solution. Analysis of the Bode phase plots indicate similar insights to the Bode Gain plots. It is observed the surface appears reactive but stable for the -100 mV potential hold. There appears a relatively stable surface for 0 mV, 100 mV, and 200 mV potential holds, although the 200 mV surface may be becoming less slightly less stable with time or undulating slightly. Also, the 300 mV surface appears unstable and becoming more so with time. A -90 ° phase shift is typical of a capacitive electrical circuit element, and indicates the surface of the electrode is acting as a capacitor over the frequencies near this value.

Durability and Degradation of HT9 Based Alloy Waste Forms with Variable Ni and Cr Content
FCRD-MRWFD-2017-000407
SRNL-STI-2016-00719
December 31, 2016

33
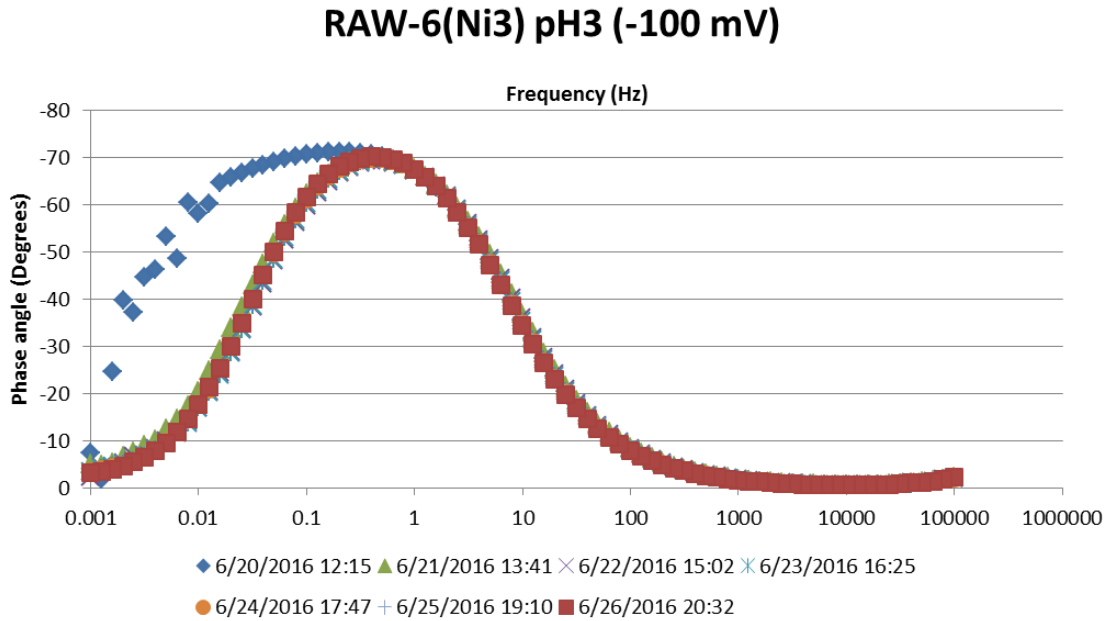
Figure 20 Bode phase plot for -100 mV potentiostatic EIS in alkaline brine for the RAW-6(Ni3) alloy electrode.
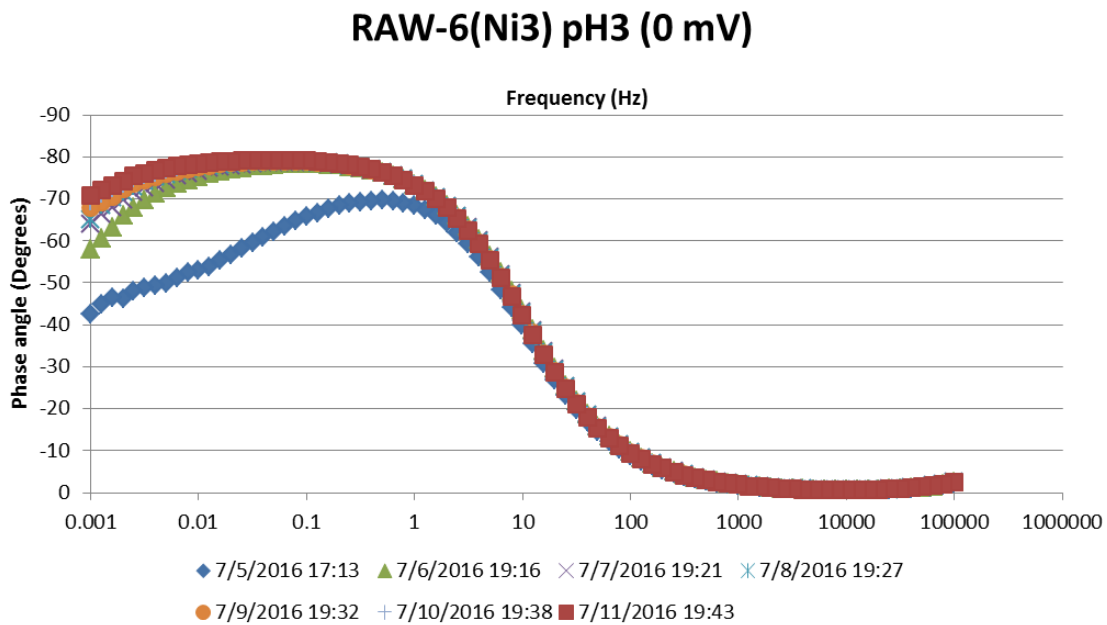
Figure 21 Bode phase plot for 0 mV potentiostatic EIS in alkaline brine for the RAW-6(Ni3) alloy electrode.

Durability and Degradation of HT9 Based Alloy Waste Forms with Variable Ni and Cr Content
FCRD-MRWFD-2017-000407
SRNL-STI-2016-00719
December 31, 2016

34

RAW-6(Ni3) pH3 (100 mV)
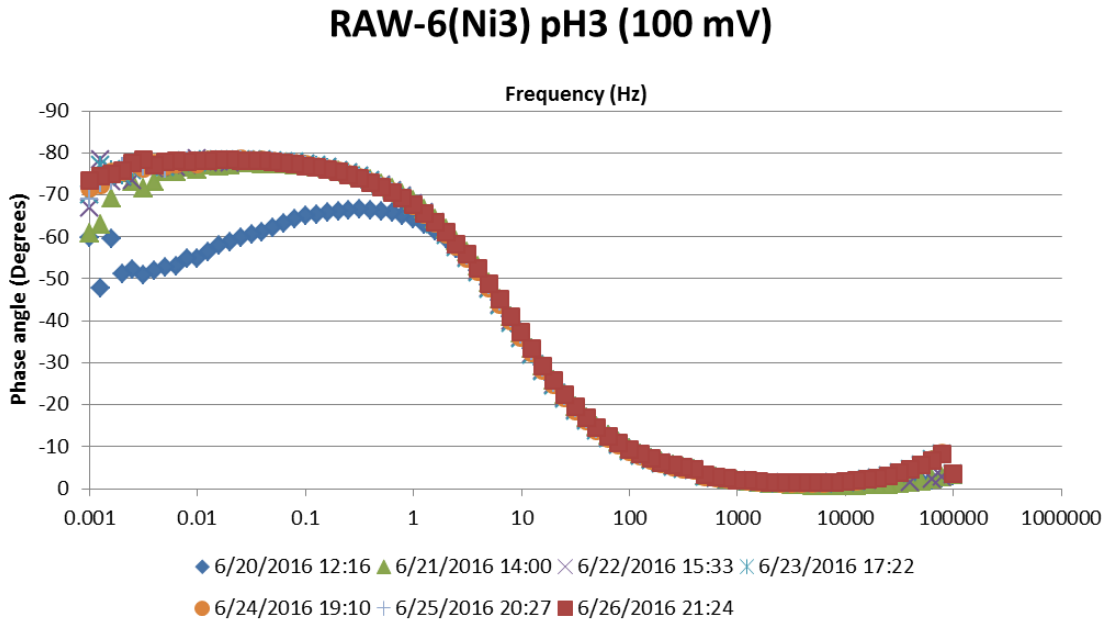
Figure 22 Bode phase plot for 100 mV potentiostatic EIS in alkaline brine for the RAW-6(Ni3) alloy electrode.

RAW-6(Ni3) pH3 (200 mV)
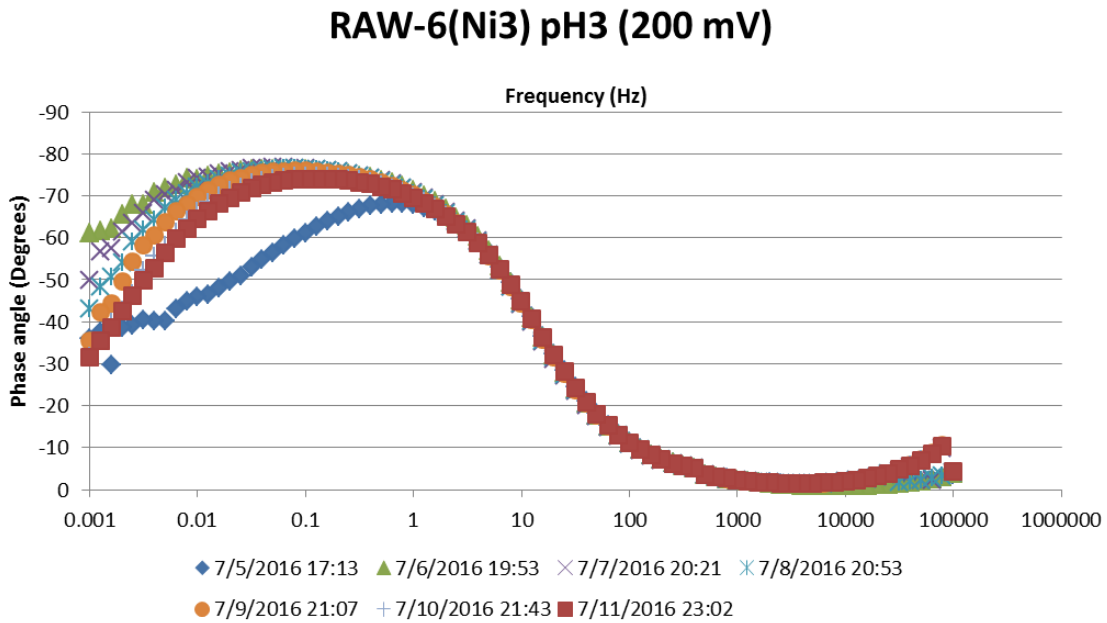
Figure 23 Bode phase plot for 200 mV potentiostatic EIS in alkaline brine for the RAW-6(Ni3) alloy electrode.

Durability and Degradation of HT9 Based Alloy Waste Forms with Variable Ni and Cr Content
FCRD-MRWFD-2017-000407
SRNL-STI-2016-00719
December 31, 2016

35
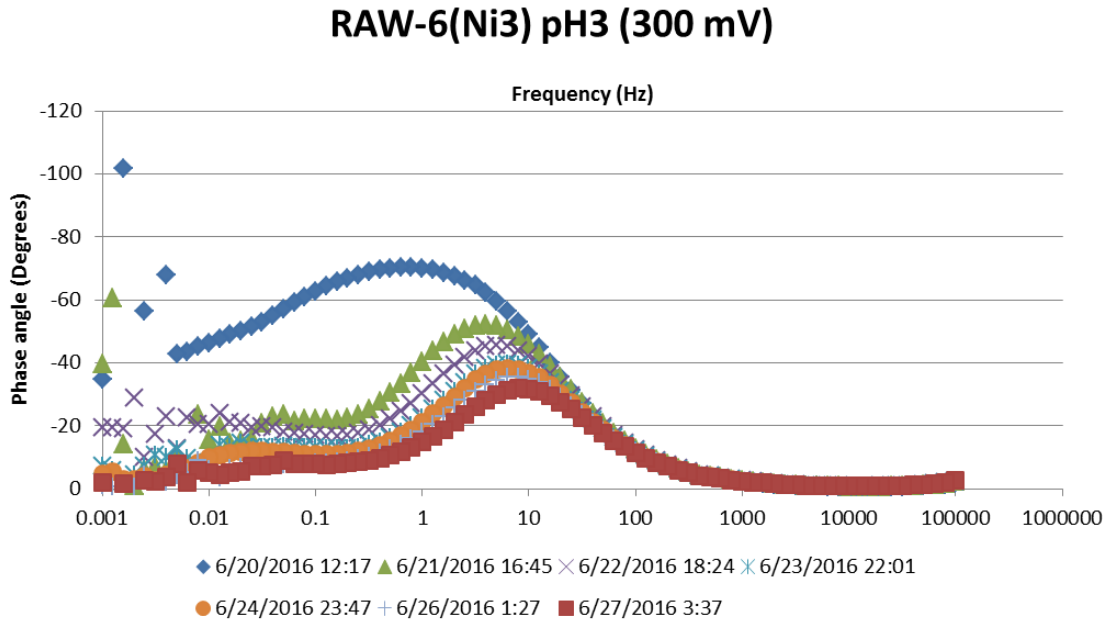
Figure 24 Bode phase plot for 300 mV potentiostatic EIS in alkaline brine for the RAW-6(Ni3) alloy electrode.

3.3.2   Nyquist Plots

The Nyquist plots, Figure 25 through Figure 29, can indicate if a protective oxidation layer was forming and the degree to which it is protective. In Figure 25, it is seen by the decrease in the intercept of the semicircle lines formed by each curve, that the surface lost its passivation layer and then held at a constant value. For the 0 mV and 100 mV potential holds, Figure 26, Figure 27, respectively, the assumed semi-circle intercept appears to increase in value (although the intercept is not observed due to lack of data at values near where this intercept would occur), indicating that a passivation layer is increasingly becoming more stable. In Figure 28, the surface appears to reach a maximum passivation by the second day and then starts to decrease in its impedance. In Figure 29 it is observed that the surface loses some passivity early on, and then gradually loses impedance.   Because different phases can have different reaction layers that respond differently to EIS, data interpretation can be difficult.

Durability and Degradation of HT9 Based Alloy Waste Forms with Variable Ni and Cr Content
FCRD-MRWFD-2017-000407
SRNL-STI-2016-00719
December 31, 2016

36
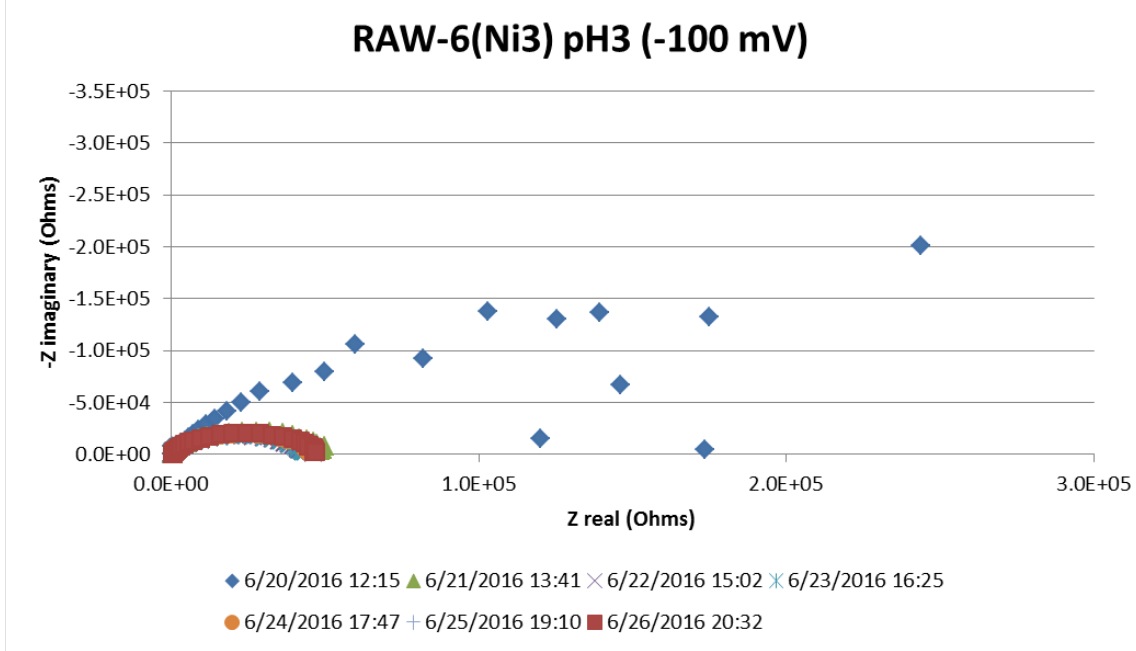
Figure 25 Nyquist plot for -100 mV potentiostatic EIS in alkaline brine for the RAW-6(Ni3) alloy electrode.
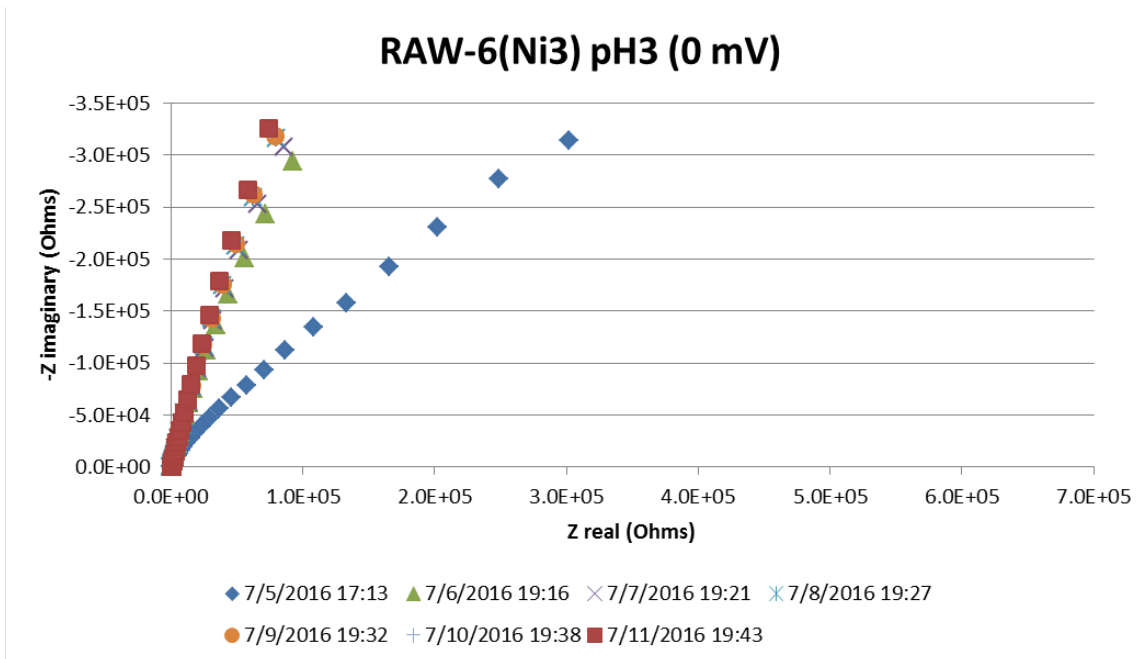
Figure 26 Nyquist plot for 0 mV potentiostatic EIS in alkaline brine for the RAW-6(Ni3) alloy electrode.
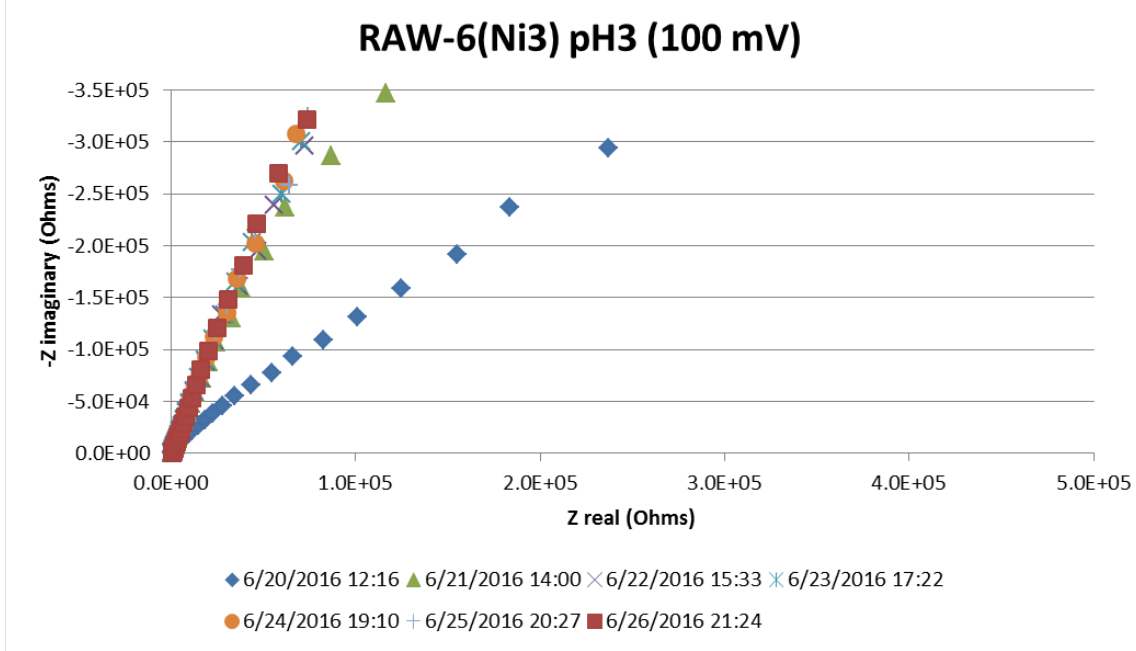
Figure 27 Nyquist plot for 100 mV potentiostatic EIS in alkaline brine for the RAW-6(Ni3) alloy electrode.
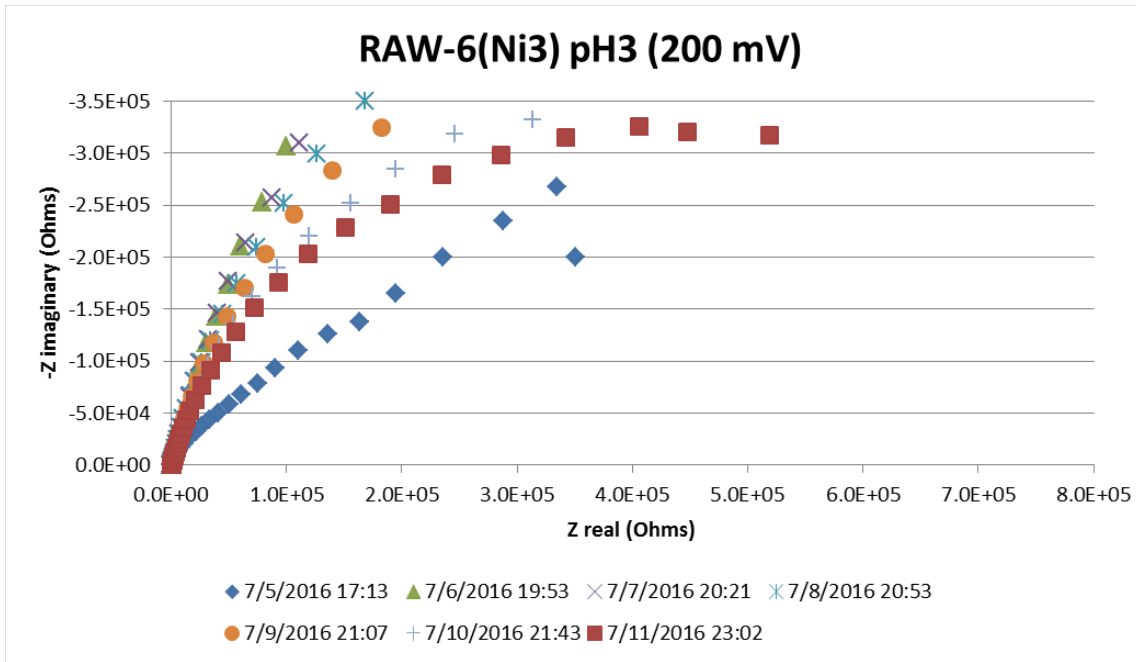
Figure 28 Nyquist plot for 200 mV potentiostatic EIS in alkaline brine for the RAW-6(Ni3) alloy electrode.

Durability and Degradation of HT9 Based Alloy Waste Forms with Variable Ni and Cr Content
FCRD-MRWFD-2017-000407
SRNL-STI-2016-00719
December 31, 2016

38
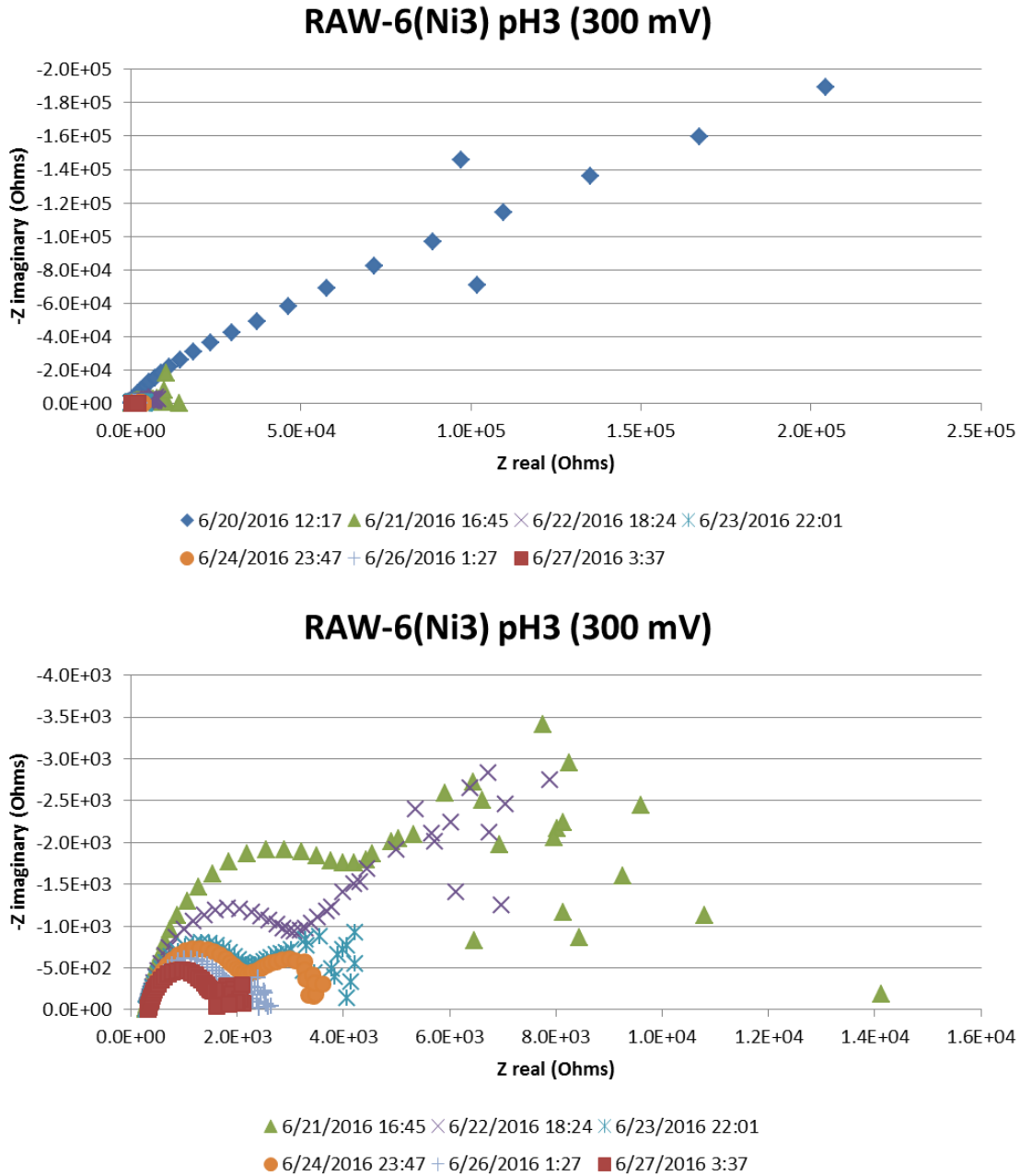
Figure 29 Nyquist plots for 300 mV potentiostatic EIS in alkaline brine for the RAW-6(Ni3) alloy electrode. In the upper plot, the first day data is platted, and it is not plotted in the lower plot.

3.4 E_{Corr} Evolution

Two electrodes made from alloy RAW-6(Ni3) were held at a series of increasingly oxidative potentials to determine how rapidly the electrode surface corrosion potential (E_{Corr}) shifts after test initialization. The potential holds started at -450 mV vs SCE (after a 2 min hold at -500 mV), and proceeded to 150 mV, in 50 mV steps. Each potential step was held for 1 hour and the current recorded. Figure 30 and Figure 31 show that both electrodes exhibited a shift from oxidation to reduction within the first hour at a potential of -400 mV vs. SCE. The results of

these tests indicated a much more negative potential for the shift from oxidation to reduction than that observed from the -100 mV data (Figure 10), which had the first consistent shifts to reducing conditions within the first hour of exposure.
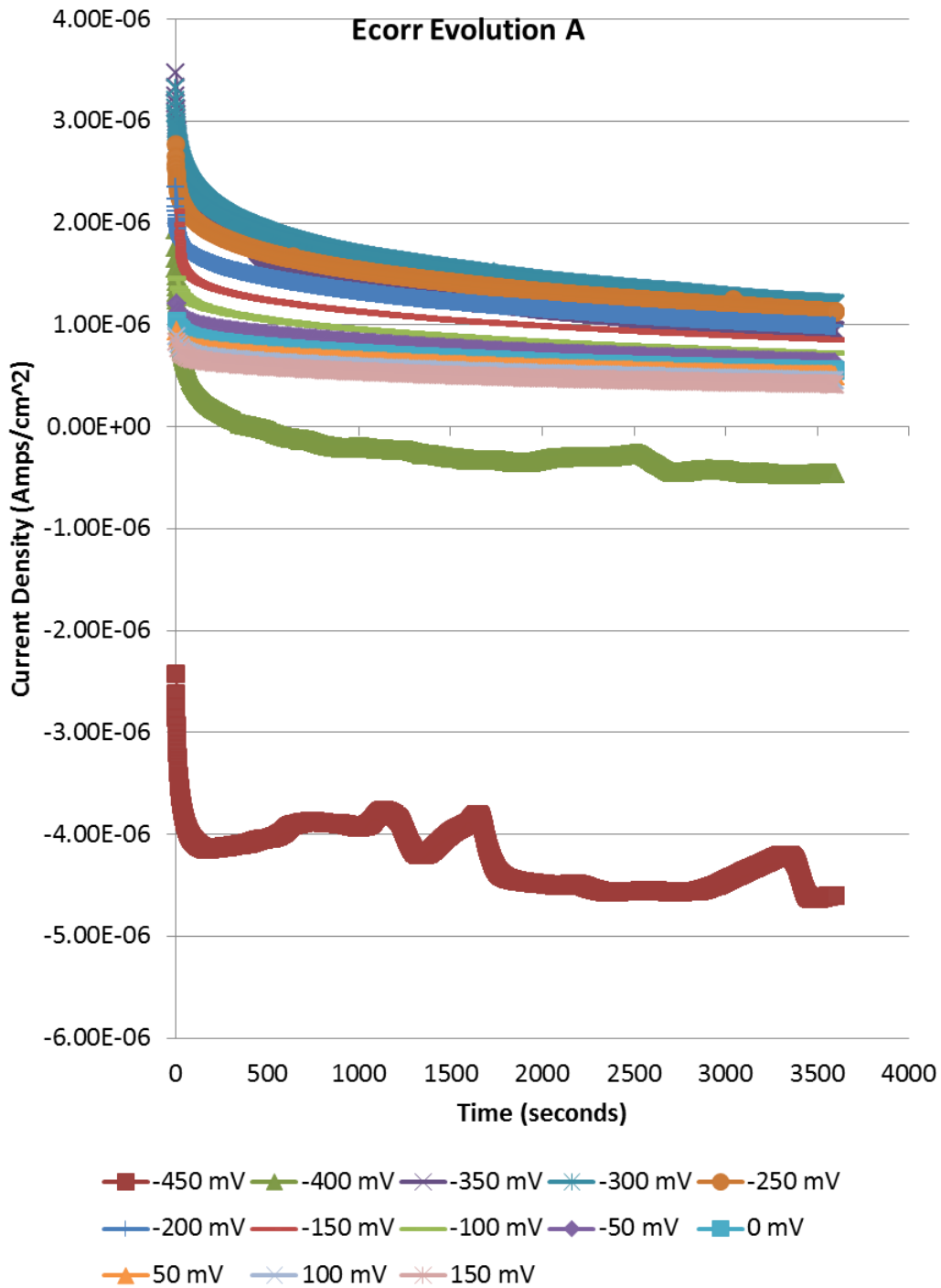
Figure 30 Current densities plotted as functions of elapsed time for an electrode made from electrode A of alloy RAW-6(Ni3). The -400 mV vs. SCE starts in an oxidative position, and then becomes reducing after about 430 seconds.
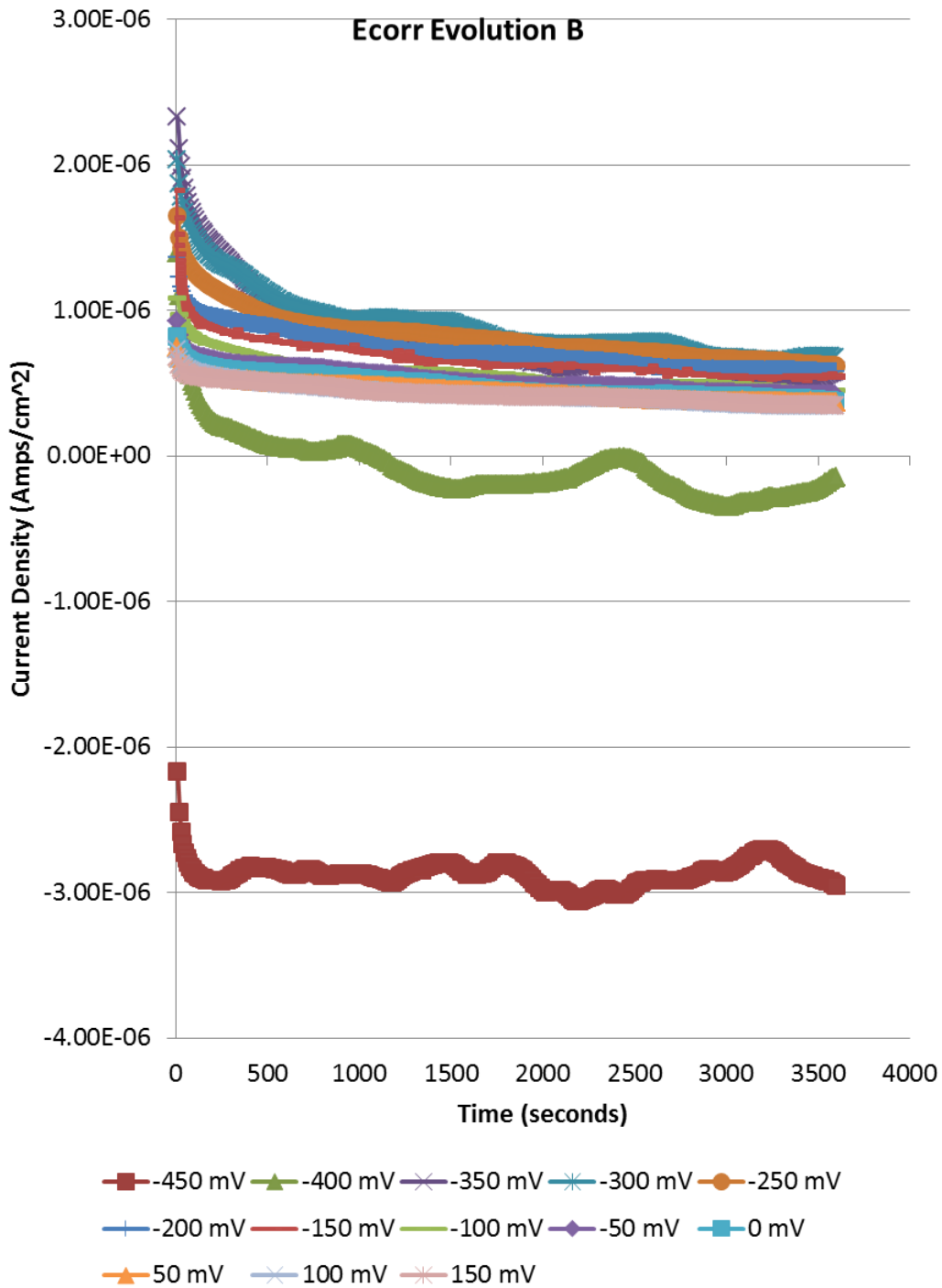
Figure 31 Current densities plotted as functions of elapsed time for an electrode made from electrode B of alloy RAW-6(Ni3). The -400 mV vs. SCE starts in an oxidative position, and then becomes reducing after about 1100 seconds.

3.5   Post Exposure SEM

The RAW-6(Ni1), RAW-6(Ni3), and RAW-6(Ni5) electrodes were evaluated by SEM after the bare surface potentiodynamic characterization, and the RAW-6(Ni3) electrodes were examined via SEM after each hybrid test. Only the hybrid test at the 300 mV hold potential showed a change to its morphology after the testing however, so it is the only hybrid test that will be discussed in this report. The bare surface potentiodynamic scans subjected the alloys to more aggressive oxidative potentials, and the electrodes showed more evidence of pitting/crevice corrosion, so more emphasis in the SEM analysis is given to this data.

3.5.1   pH 3 Bare Surface Post Exposure SEM

Figure 32, Figure 33, and Figure 34 show the RAW-6(Ni1), RAW-6(Ni3), and RAW-6(Ni5) alloy electrodes pre and post exposure to pH 3 acidic brine and the potentiodynamic scan up to 1000 mV vs SCE. Increased attack at crevices may have occurred, and localized corrosion is apparent, with attack appearing to be concentrated on the $ZrFe_2$ phase.
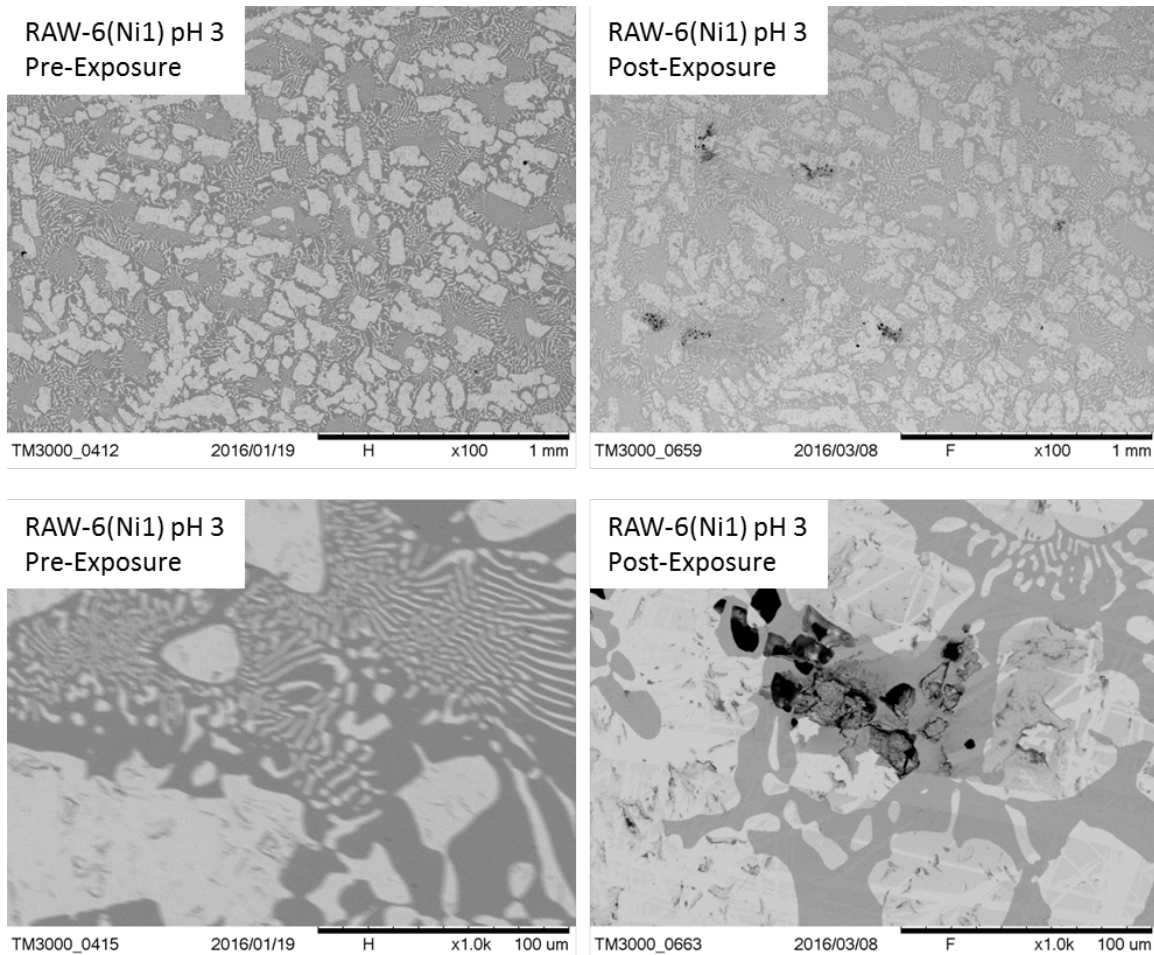
Figure 32 SEM images from the RAW-6(Ni1) alloy electrode after exposure to pH 3 and oxidative potentials during the bare surface potentiodynamic scan. Note: High magnification images are not of the same area.

Durability and Degradation of HT9 Based Alloy Waste Forms with Variable Ni and Cr Content
FCRD-MRWFD-2017-000407
SRNL-STI-2016-00719
December 31, 2016

42
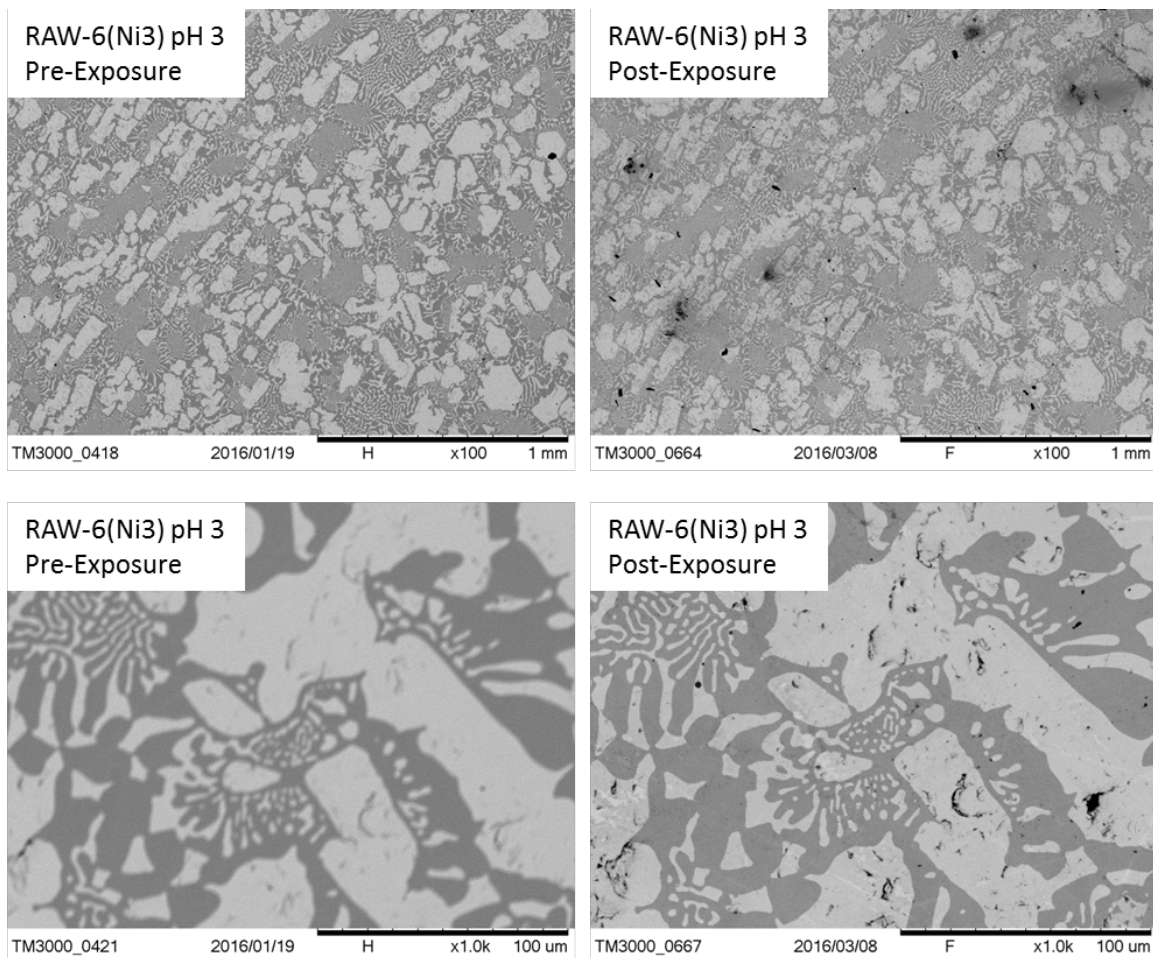
Figure 33 SEM images from the RAW-6(Ni3) alloy electrode after exposure to pH 3 and oxidative potentials during the bare surface potentiodynamic scan.
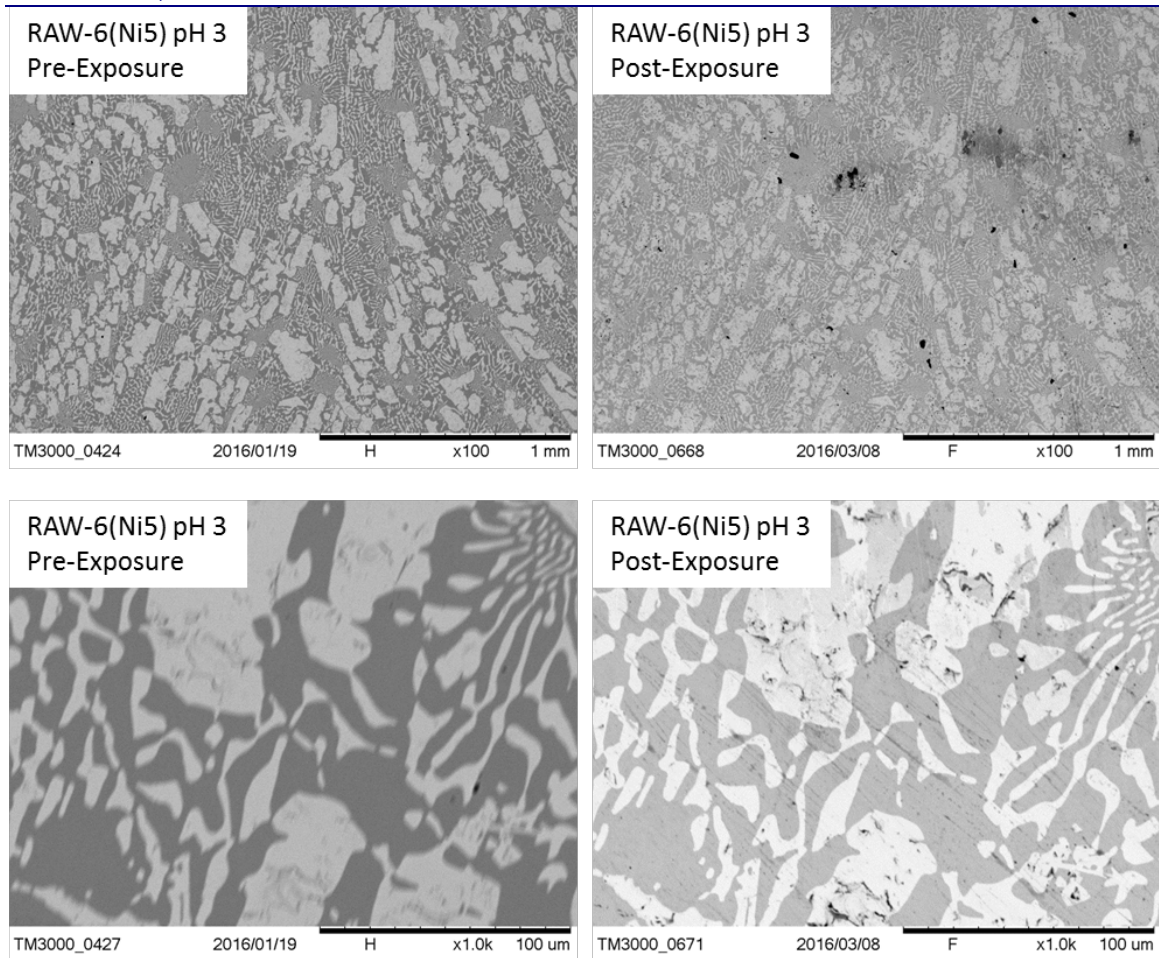
Figure 34 SEM images from the RAW-6(Ni5) alloy electrode after exposure to pH 3 and oxidative potentials during the bare surface potentiodynamic scan.

3.5.2   pH 5 Bare Surface Post Exposure SEM

Figure 35, Figure 36, and Figure 37 show the RAW-6(Ni1), RAW-6(Ni3), and RAW-6(Ni5) alloy electrodes pre and post exposure to pH 5 acidic brine and the potentiodynamic scan up to 1000 mV vs SCE. Increased attack at crevices may have occurred, and localized corrosion is apparent, with attack appearing to be concentrated on the $ZrFe_2$ phase.
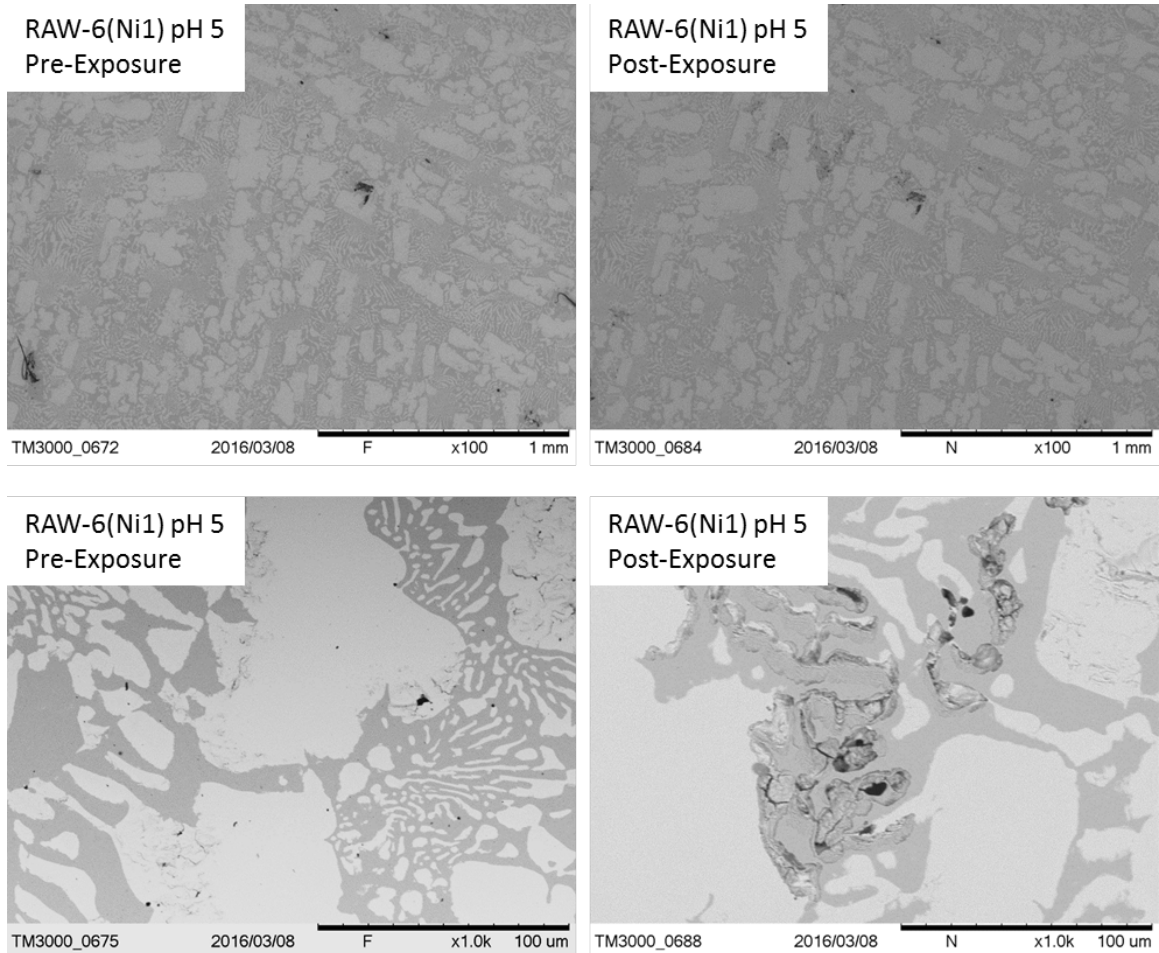
Figure 35 SEM images from the RAW-6(Ni1) alloy electrode after exposure to pH 5 and oxidative potentials during the bare surface potentiodynamic scan. Note: High magnification images are not of the same area.
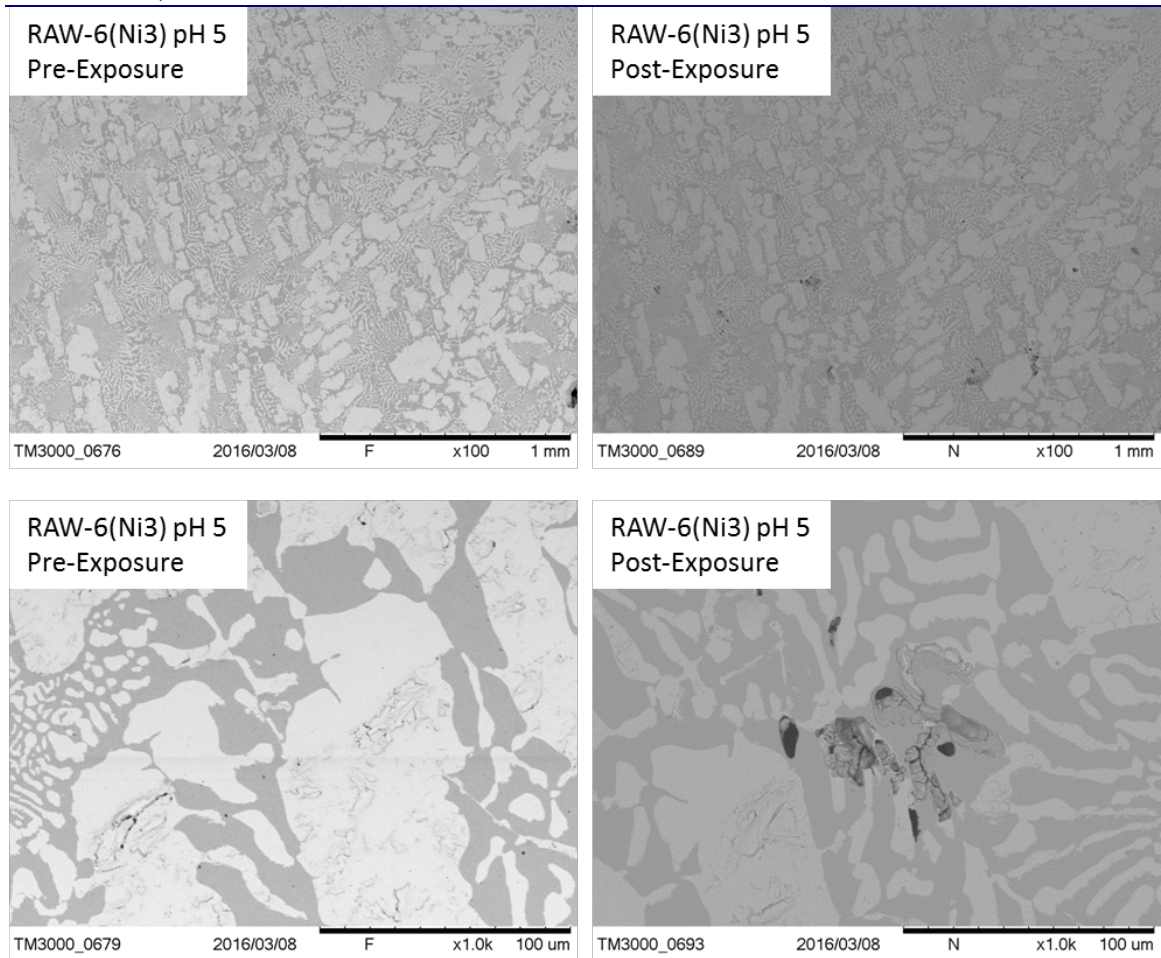
Figure 36 SEM images from the RAW-6(Ni3) alloy electrode after exposure to pH 5 and oxidative potentials during the bare surface potentiodynamic scan. Note: High magnification images are not of the same area.
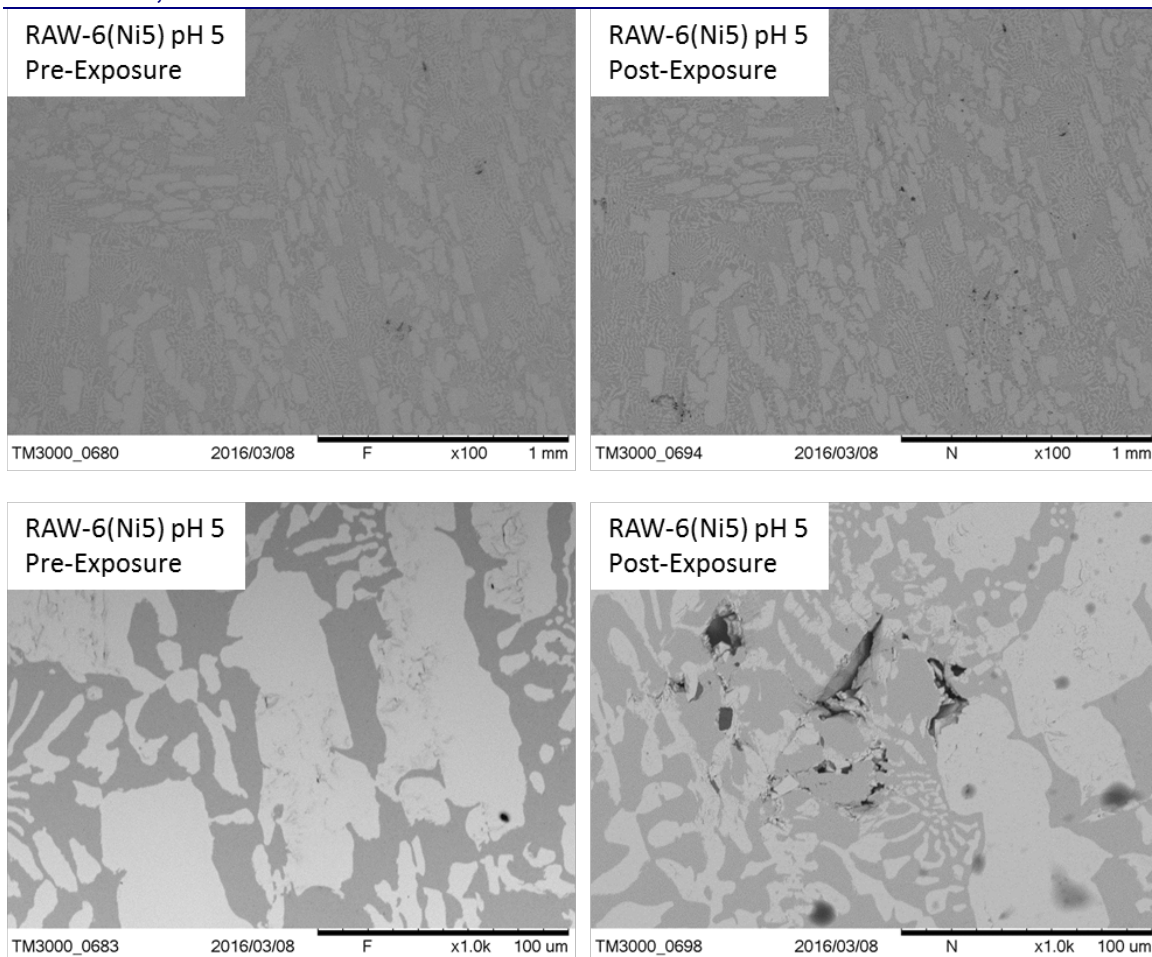
Figure 37 SEM images from the RAW-6(Ni5) alloy electrode after exposure to pH 5 and oxidative potentials during the bare surface potentiodynamic scan. Note: High magnification images are not of the same area.

3.5.3   pH 8 Bare Surface Post Exposure SEM

Figure 38, Figure 39, and Figure 40 show the RAW-6(Ni1), RAW-6(Ni3), and RAW-6(Ni5) alloy electrodes pre and post exposure to pH 8 alkaline brine and the potentiodynamic scan up to 1000 mV vs SCE. Increased attack at crevices may have occurred, and localized corrosion is apparent, with attack appearing to be concentrated on the $ZrFe_2$ phase.
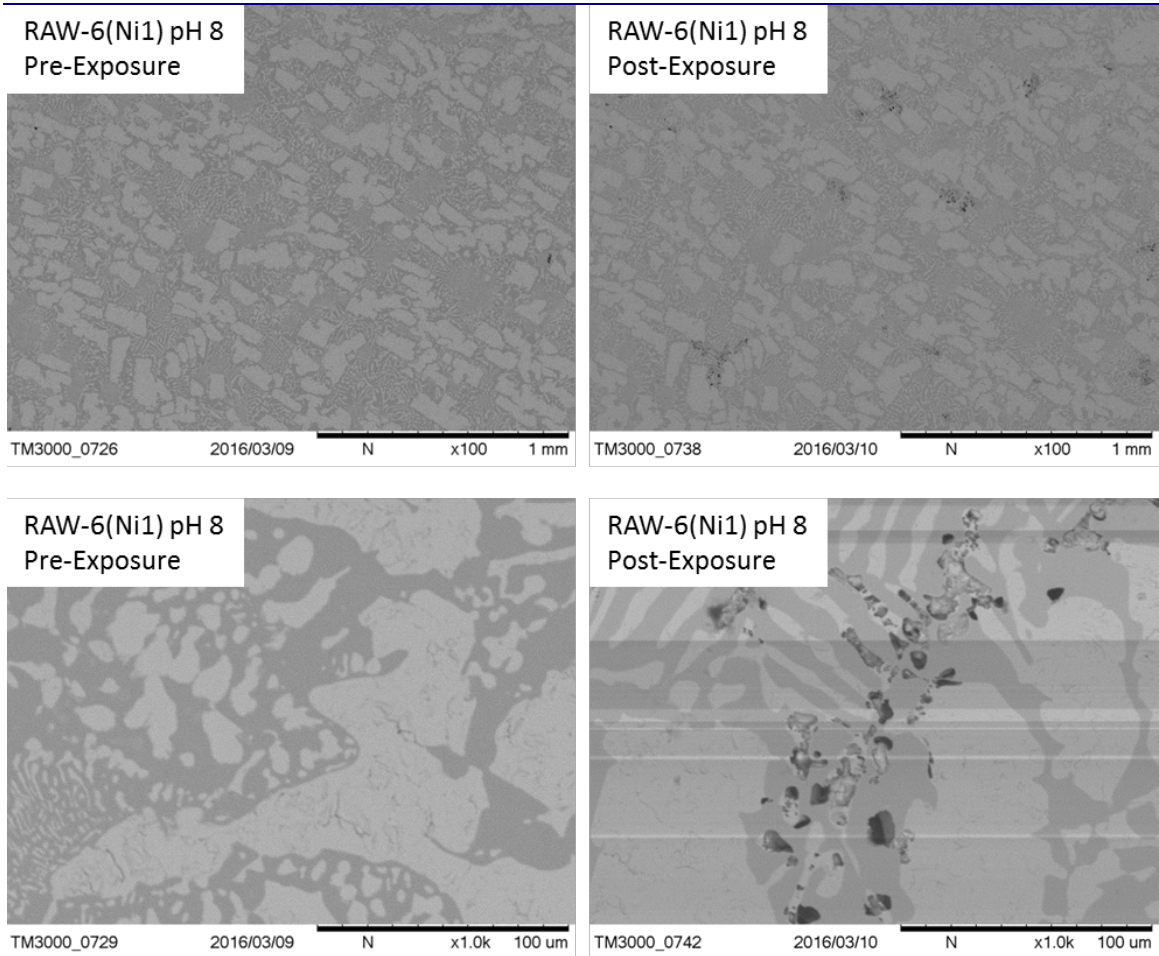
Figure 38 SEM images from the RAW-6(Ni1) alloy electrode after exposure to pH 8 and oxidative potentials during the bare surface potentiodynamic scan. Note: High magnification images are not of the same area.
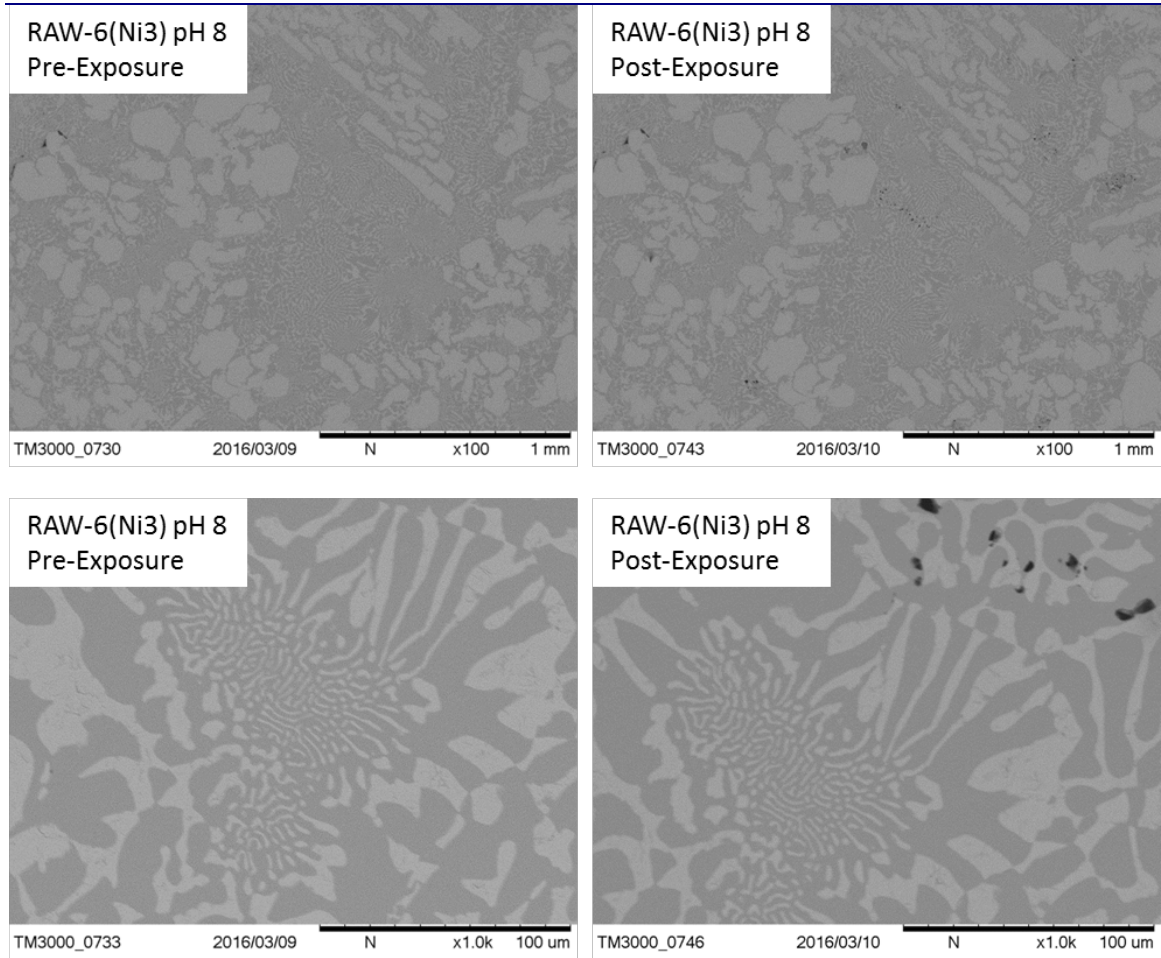
Figure 39 SEM images from the RAW-6(Ni3) alloy electrode after exposure to pH 8 and oxidative potentials during the bare surface potentiodynamic scan.
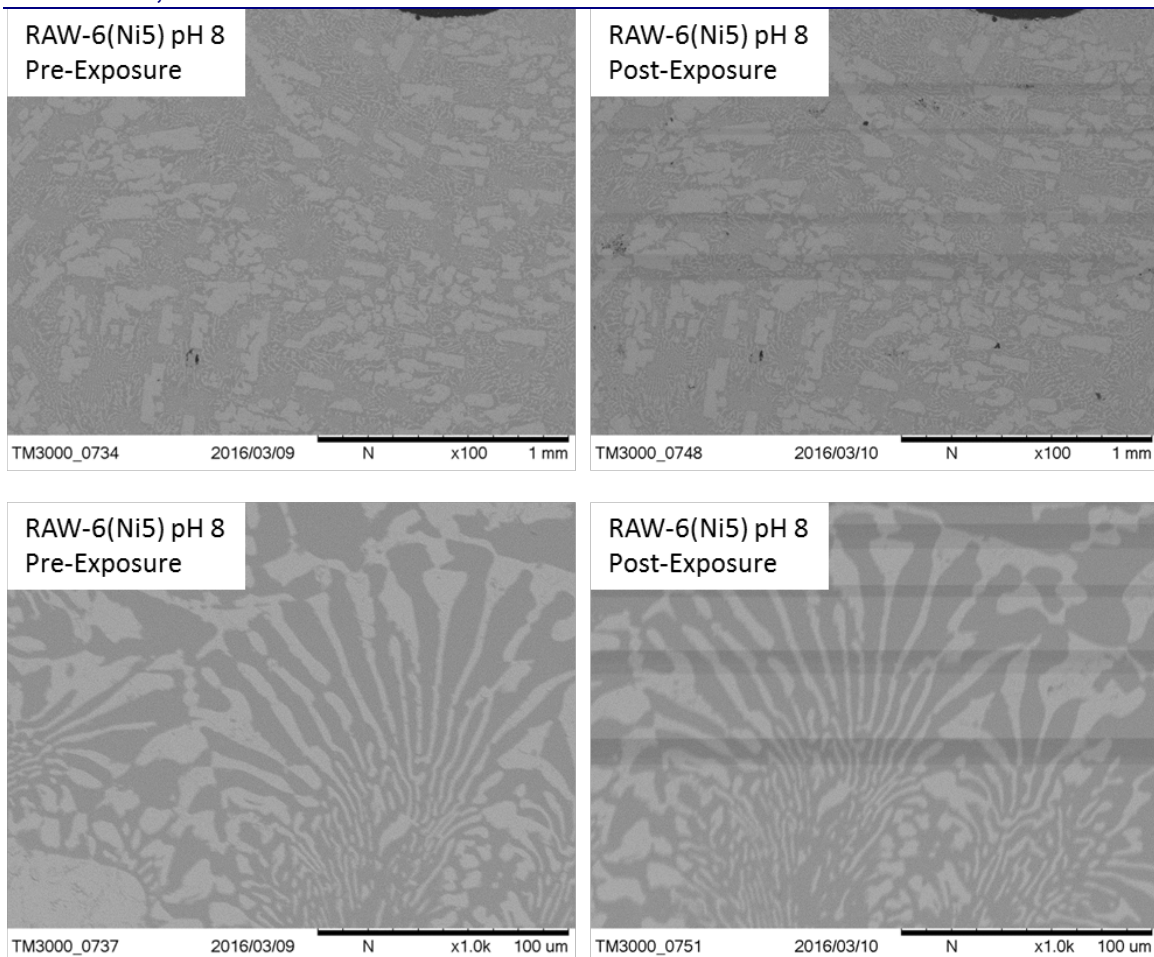
Figure 40 SEM images from the RAW-6(Ni5) alloy electrode after exposure to pH 8 and oxidative potentials during the bare surface potentiodynamic scan.

3.5.4 pH 10 Bare Surface Post Exposure SEM

Figure 41, Figure 42, and Figure 43 show the RAW-6(Ni1), RAW-6(Ni3), and RAW-6(Ni5) alloy electrodes pre and post exposure to pH 10 alkaline brine and the potentiodynamic scan up to 1000 mV vs SCE. Increased attack at crevices may have occurred, and localized corrosion is apparent, with attack appearing to be concentrated on the $ZrFe_2$ phase.
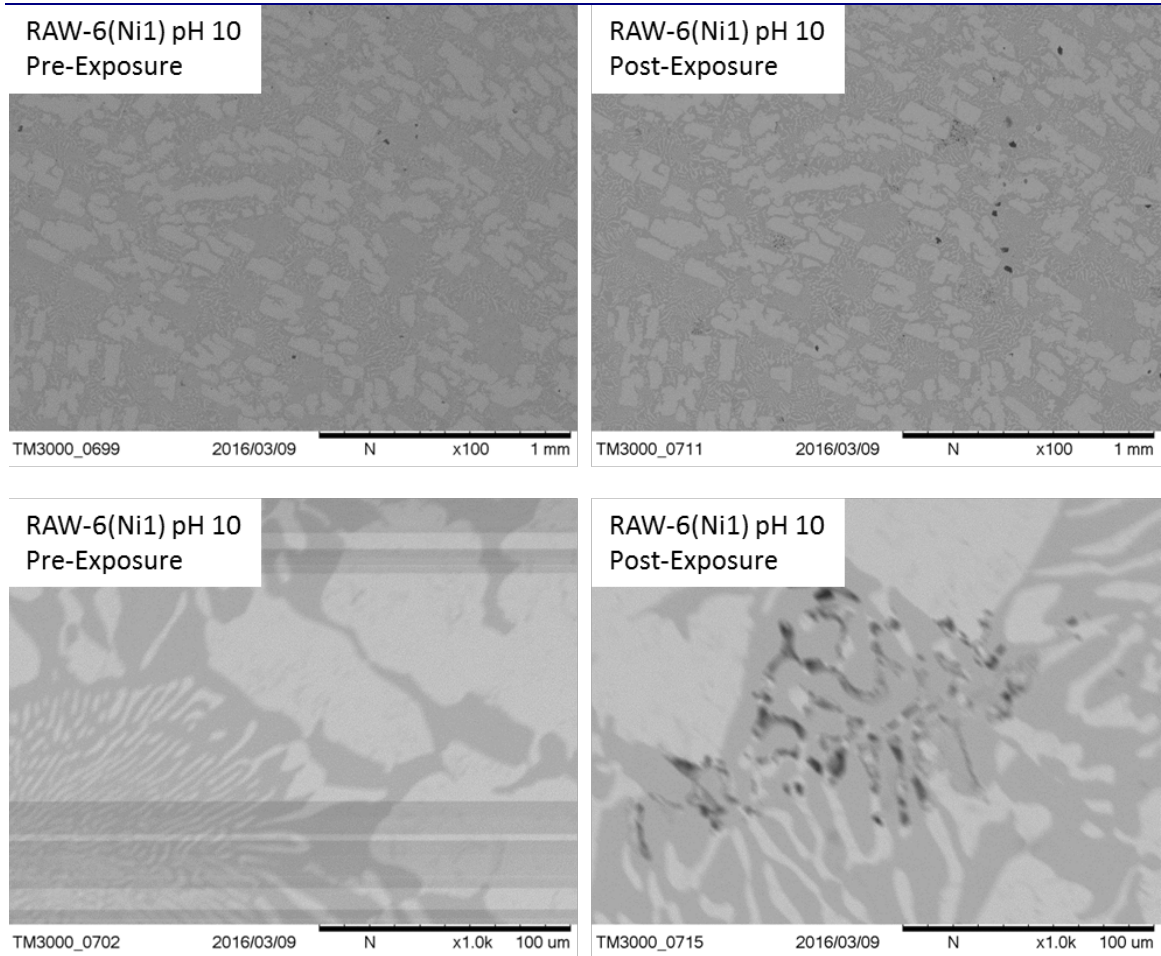
Figure 41 SEM images from the RAW-6(Ni1) alloy electrode after exposure to pH 10 and oxidative potentials during the bare surface potentiodynamic scan. Note: High magnification images are not of the same area.
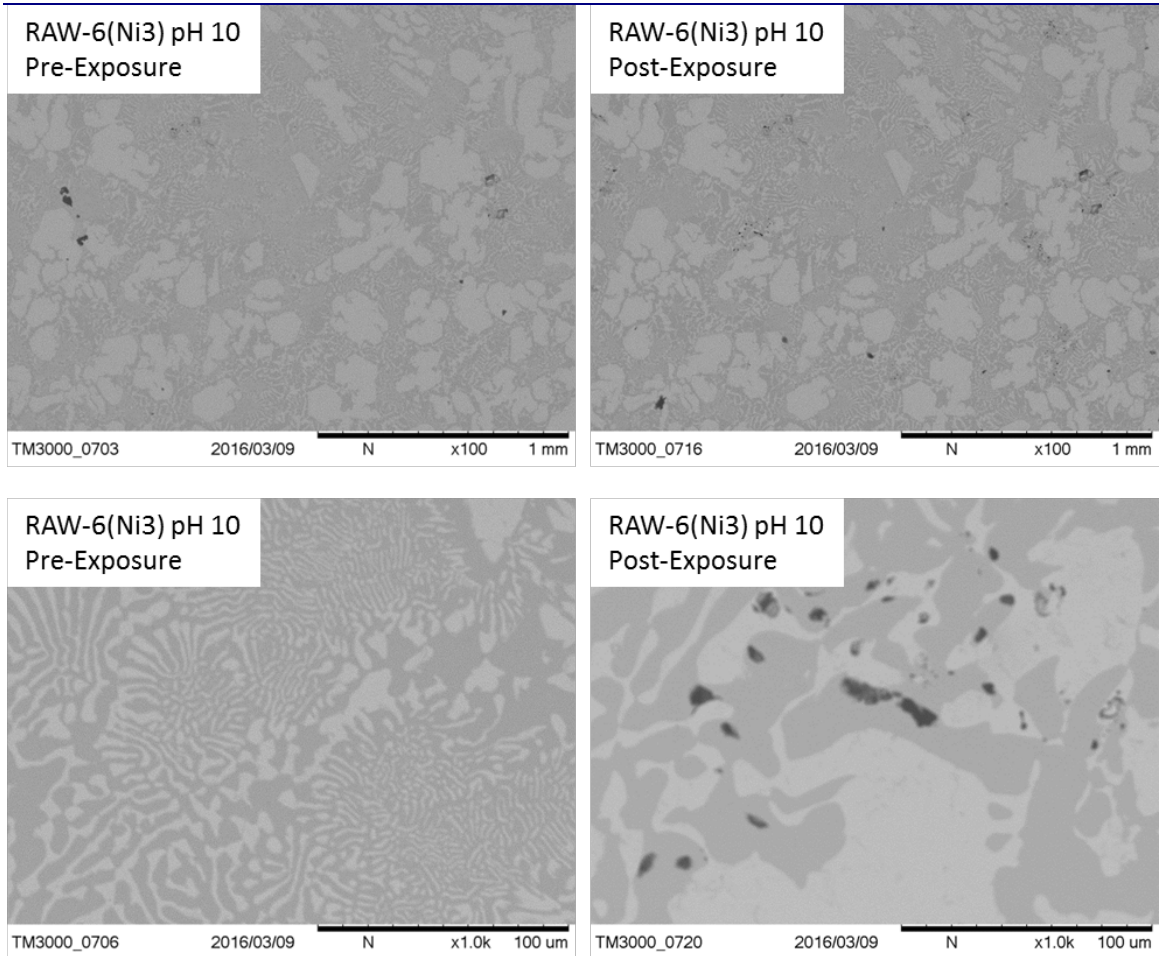
Figure 42 SEM images from the RAW-6(Ni3) alloy electrode after exposure to pH 10 and oxidative potentials during the bare surface potentiodynamic scan. Note: High magnification images are not of the same area.
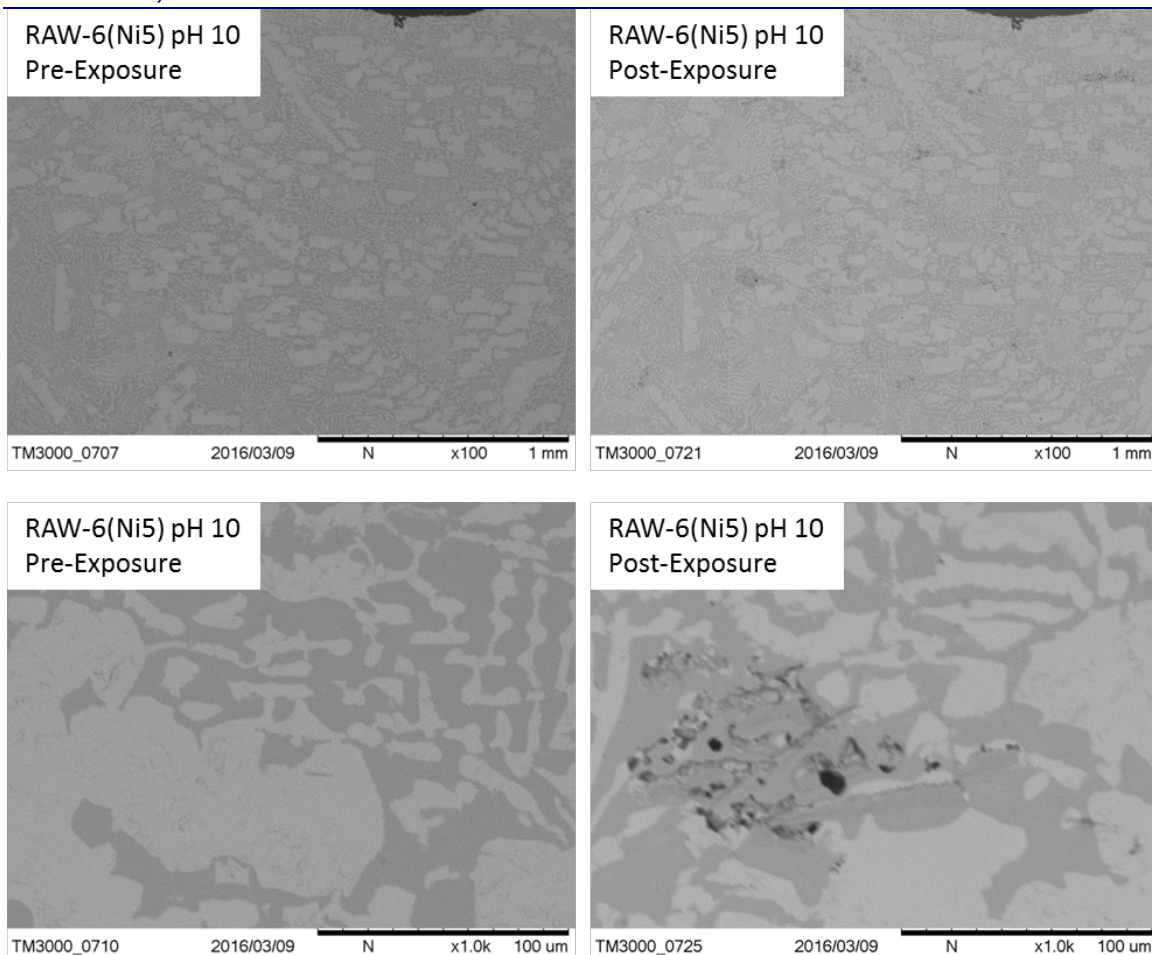
Figure 43 SEM images from the RAW-6(Ni5) alloy electrode after exposure to pH 10 and oxidative potentials during the bare surface potentiodynamic scan. Note: High magnification images are not of the same area.

3.5.5   300 mV Hybrid Post Test SEM

Figure 44 shows the before and after exposure SEM images of the RAW-6(Ni3) electrode after the 300 mV vs. SCE hybrid test potentiostatic hold. Of all the hybrid tests, this was the only one that showed noticeable degradation of the surface. The 300 mV hybrid test appeared to shift from passive to transpassive behavior over the course of the test as noted by the current density data, Figure 14. Similar to the attack visible on the bare surface alloy SEM characterizations, the attack appears to be localized to the $ZrFe_2$ phase, and potentially preferential to preexisting crevices.
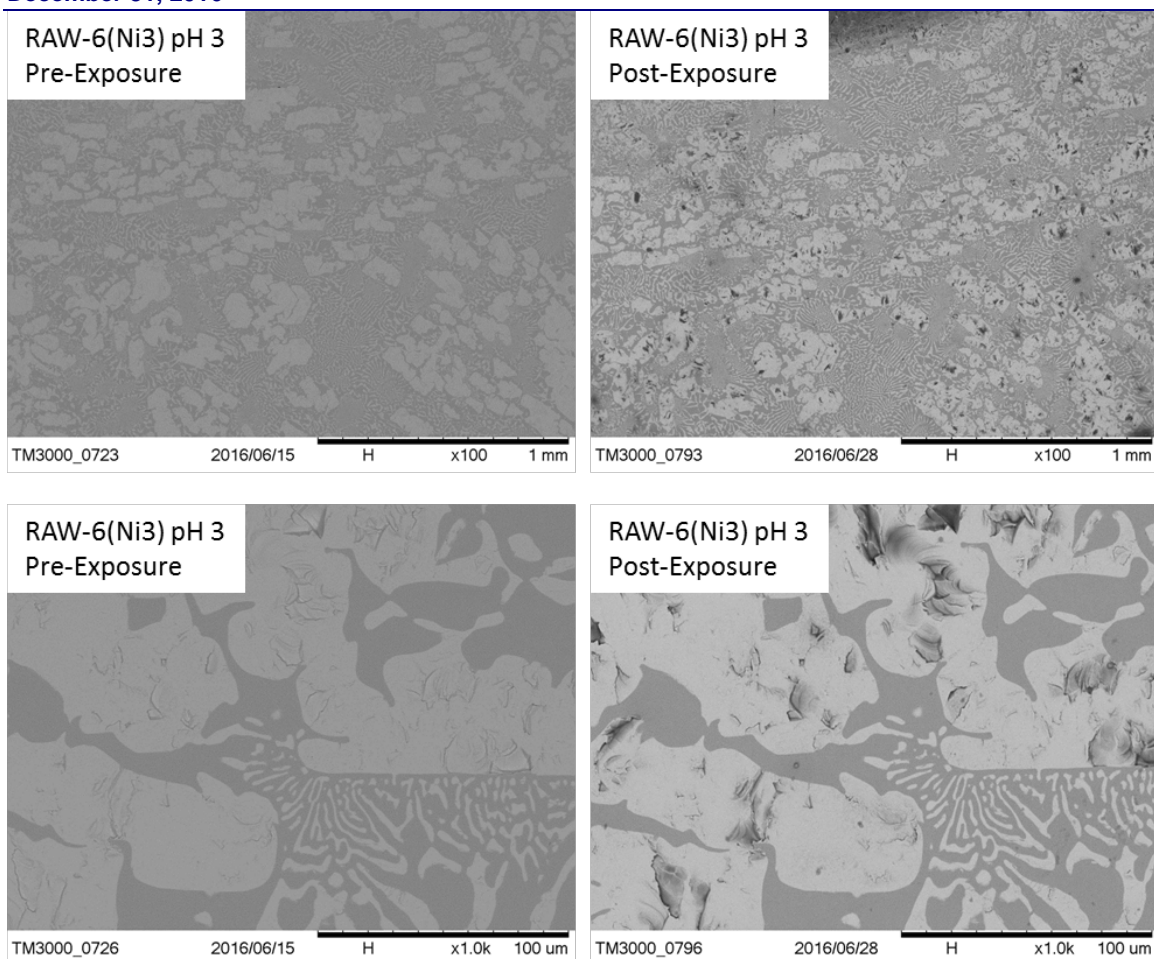
Figure 44 SEM images from the RAW-6(Ni3) alloy electrode after exposure to pH 3 and oxidative potentials during the hybrid test potentiostatic hold of 300 mV vs. SCE.

3.6   Hybrid Test Solution Analysis

Aliquots from the test solutions from the hybrid tests performed with the RAW-6(Ni3) electrode were taken and analyzed at specific points during the long-term electrochemical measurements. The following elements were analyzed for: Cr, Fe, Co, Mo, and Re. The solution elemental concentrations were divided by the exposed alloy surface area to give the total elemental release per area at each aliquot time, and can be further divided by the exposure time to give a release rate per exposed area. The solution analysis results are shown in Table 8, Table 9, Table 10, Table 11, and Table 12, and in Figure 45, Figure 46, Figure 47, and Figure 48. Notable observations include 1) the 300 mV hybrid test was the only one to consistently show increased concentrations of investigated elements over the test duration, 2) Cr and Fe had consistent decreases in solution concentrations for all hybrid tests except for the 300 mV test, and 3) only the 300 mV test had a significant increase in Re concentration as the test duration increased.

Table 8 Concentration of Cr, Fe, Co, Mo, and Re per area of exposed electrode as a function of -100 mV hybrid test duration.

-100 mV						
Exposure time (hr:min:sec)	Exposure time (UNIX)	Cr (ppb/cm²)	Fe (ppb/cm²)	Co (ppb/cm²)	Mo (ppb/cm²)	Re (ppb/cm²)
0:00:00	1466422920	2.5	32.9	0.2	0.5	0.1
21:42:00	1466501040	2.8	63.2	0.6	0.5	0.1
68:58:00	1466671200	2.3	39.1	0.3	0.5	0.1
165:01:00	1467016980	2.3	31.7	0.3	0.5	0.1

Table 9 Concentration of Cr, Fe, Co, Mo, and Re per area of exposed electrode as a function of 0 mV hybrid test duration.

0 mV						
Exposure time (hr:min:sec)	Exposure time (UNIX)	Cr (ppb/cm²)	Fe (ppb/cm²)	Co (ppb/cm²)	Mo (ppb/cm²)	Re (ppb/cm²)
0:00:00	1467737460	1.4	18.4	0.3	0.3	0.1
21:10:00	1467813660	2.0	31.1	0.5	0.4	0.1
69:56:00	1467989220	1.8	23.8	0.4	0.5	0.1
162:29:00	1468322400	1.8	34.2	0.4	0.5	0.1

Table 10 Concentration of Cr, Fe, Co, Mo, and Re per area of exposed electrode as a function of 100 mV hybrid test duration.

100 mV						
Exposure time (hr:min:sec)	Exposure time (UNIX)	Cr (ppb/cm²)	Fe (ppb/cm²)	Co (ppb/cm²)	Mo (ppb/cm²)	Re (ppb/cm²)
0:00:00	1466422920	9.3	39.8	0.2	1.2	0.1
21:43:00	1466501100	9.8	49.5	0.3	0.7	0.1
69:00:00	1466671320	2.2	1.7	0.1	0.8	0.1
165:03:00	1467017100	0.5	7.3	0.1	1.7	0.1

Table 11 Concentration of Cr, Fe, Co, Mo, and Re per area of exposed electrode as a function of 200 mV hybrid test duration.

200 mV						
Exposure time (hr:min:sec)	Exposure time (UNIX)	Cr (ppb/cm²)	Fe (ppb/cm²)	Co (ppb/cm²)	Mo (ppb/cm²)	Re (ppb/cm²)
0:00:00	1467737460	8.4	58.8	0.2	0.7	0.1
21:12:00	1467813780	8.1	70.4	0.1	0.5	0.1
69:59:00	1467989400	5.5	25.7	0.2	0.5	0.1
162:31:00	1468322520	1.1	1.2	0.1	0.7	0.1

Table 12 Concentration of Cr, Fe, Co, Mo, and Re per area of exposed electrode as a function of 300 mV hybrid test duration.

300 mV						
Exposure time (hr:min:sec)	Exposure time (UNIX)	Cr (ppb/cm²)	Fe (ppb/cm²)	Co (ppb/cm²)	Mo (ppb/cm²)	Re (ppb/cm²)
0:00:00	1466422920	13.6	59.1	0.2	1.0	0.1
21:44:00	1466501160	26.6	132.9	0.4	2.0	0.4
69:01:00	1466671380	11.0	232.5	0.3	2.1	11.2
165:04:00	1467017160	616.4	3658.0	0.2	59.3	84.5
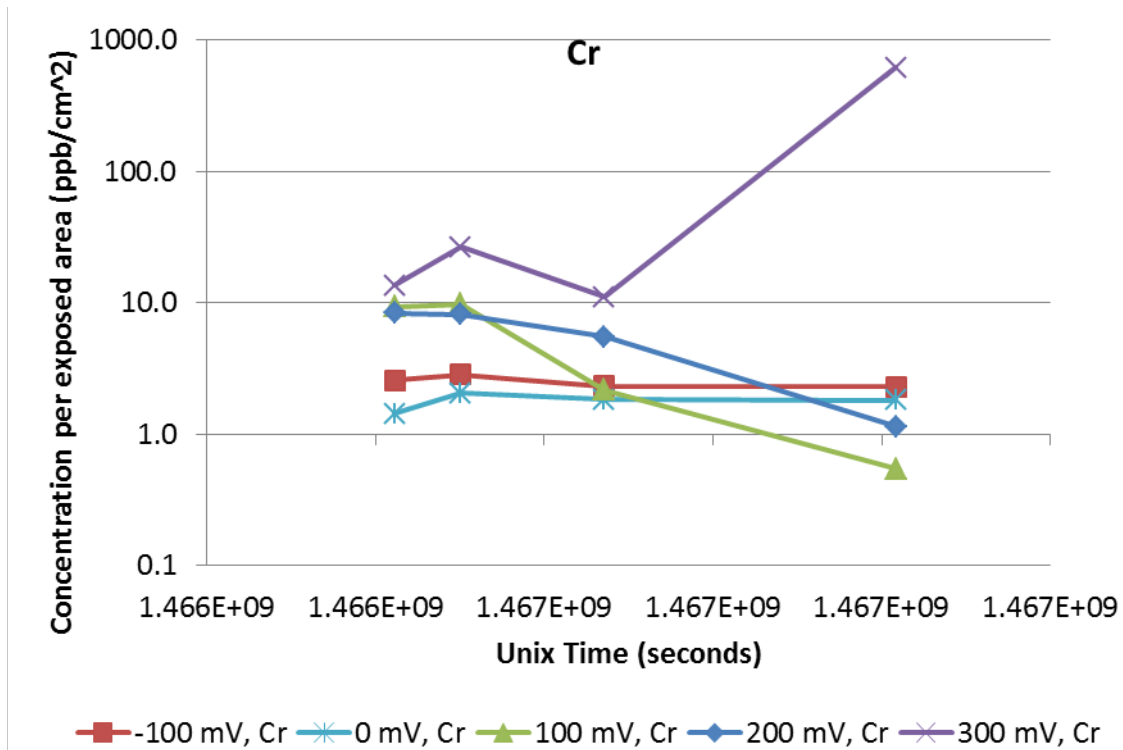
Figure 45 Cr solution analysis from the hybrid tests at pH 3 for RAW-6(Ni3) at several different hold potentials.
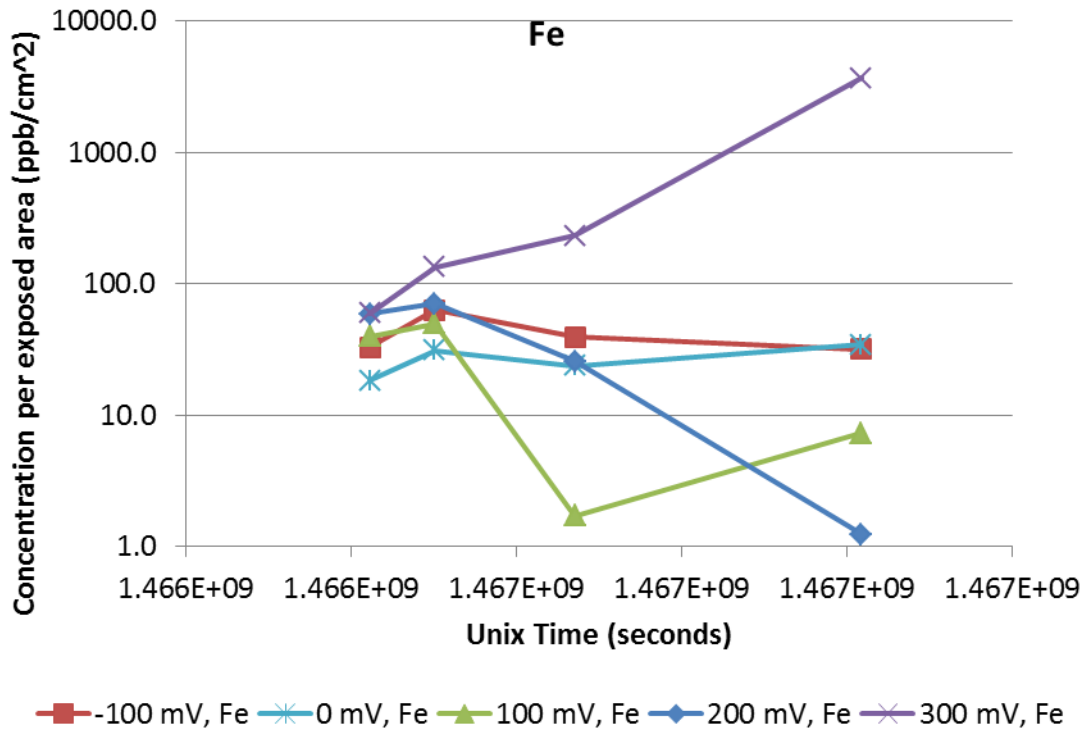
Figure 46 Fe solution analysis from the hybrid tests at pH 3 for RAW-6(Ni3) at several different hold potentials.
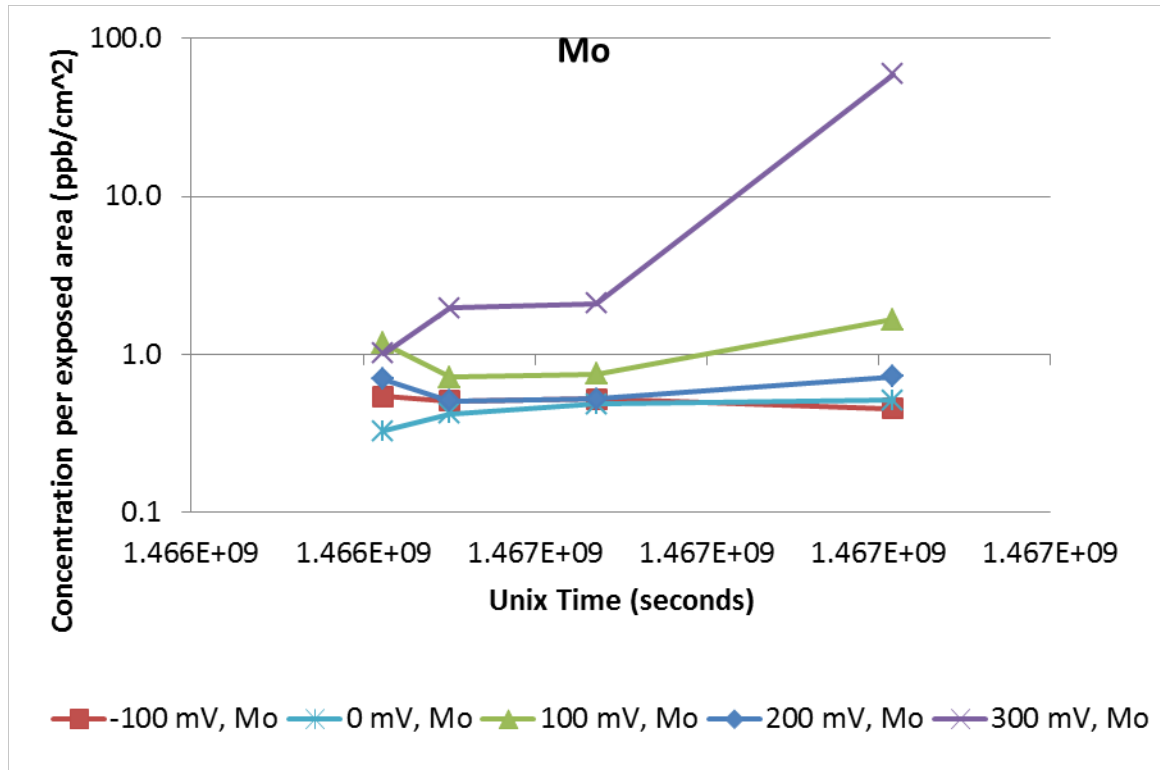
Figure 47 Mo solution analysis from the hybrid tests at pH 3 for RAW-6(Ni3) at several different hold potentials.
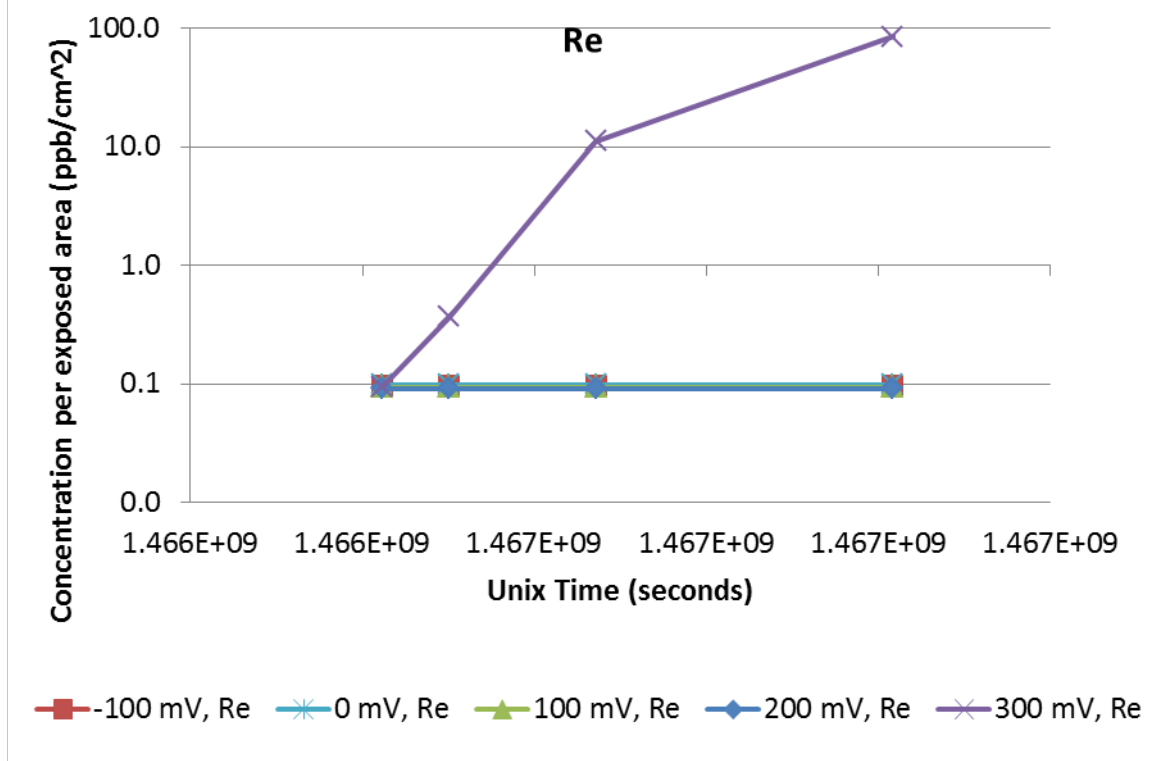
Figure 48 Re solution analysis from the hybrid tests at pH 3 for RAW-6(Ni3) at several different hold potentials.

4.   CONCLUSIONS

Surrogate alloy waste forms of the RAW-6 composition were fabricated with Ni and Cr trim additions to investigate if these elements would reduce corrosion. The alloys have an added Ni:Cr ratio of 0:0, 1:3, 3:2, and 5:1, and were given a naming scheme based on the added Ni content of RAW-6(Ni1), RAW-6(Ni3), and RAW-6(Ni5), respectively. After initial characterization by SEM and EDS, the alloys were made into electrodes and examined electrochemically in alkaline and acidic brines titrated to pH 3, 5, 8, and 10. After initial characterization of the different alloy formulations, the RAW-6(Ni3) alloy was chosen for further investigation using a hybrid test method. The hybrid test approach was developed in collaboration with Argonne National Laboratory, and consisted of 4 main steps, 1) measure the bare surface corrosion behavior in reference solutions at open circuit over a wide imposed potential range, 2) perform several differing potentiostatic holds to measure the time-evolution of anodic current, evolution of surface properties, and radionuclide concentrations in solution, 3) relate steady-state current to radionuclide (or surrogate) release rates through periodic sampling of test electrolyte, and 4) identify the corroding phase/phases using SEM/EDS. Step 2 lasted up to 7 days with mostly fixed electrode potential and periodic small magnitude potential interruptions for a variety of electrochemical analyses. This combined electrochemical and extended immersion testing is referred to as hybrid testing.

Electrochemical Analysis

The potentiodynamic scans on the fresh surfaces produce similar results for the three different alloys. The alloys, in all pH solution tested, would undergo a shift from passive to transpassive behavior at about 400 mV vs the saturated calomel electrode (SCE), and had E_{Corr} between -600 mV to 0 mV vs. SCE (with ~ -400 mV the most common E_{Corr}).

In the pH 3 solution for bare surface characterizations, the RAW-6(Ni3) alloy experienced E_{Corr} at the most cathodic potential, but then had lower current densities than the other alloys from between about 0 mV to 400 mV vs SCE. The RAW-6(Ni1) and RAW-6(Ni5) alloys had similar E_{Corr}, and current densities in general, although the RAW-6(Ni1) alloy had the highest current densities on approach to the transpassive region.

The pH 5 solution results for bare surface characterizations were similar to the pH 3 results, except that the E_{Corr} was shifted closer to -400 mV vs SCE for all alloys. The RAW-6(Ni3) alloy experienced E_{Corr} at the most cathodic potential. The RAW-6(Ni3) and RAW-6(Ni5) alloys had similar corrosion currents between 0 mV to 400 mV vs SCE, and the RAW-6(N1) alloy had slightly larger current densities than the other two alloys in this potential range.

At pH 8 the RAW-6(Ni3) and RAW-6(Ni5) current densities are virtually identical over the scan range of -500 mV to 1000 mV vs SCE. The RAW-6(Ni1) alloy had slightly higher current densities from ~0 mV until the start of the transpassive region at ~300 mV.

At pH 10 the RAW-6(Ni1) and RAW-6(Ni3) alloys both have similar E_{Corr} values, which were more cathodic than the RAW-6(Ni5). Over the majority of the passive regime, the current density of RAW-6(Ni1) was higher than that of RAW-6(Ni3), which was higher than that of RAW-6(Ni5).

The hybrid testing results for the RAW-6(Ni3) alloy indicate that at pH 3 in brine, this alloys passive region becomes more narrow in potential with time, that is, the E_{Corr} shifts to more

oxidative potentials, and the beginning of the transpassive region shifts to slightly more cathodic potentials. The -100 mV hybrid test quickly became cathodic as evidenced by negative current densities, and the 300 mV hybrid test was transpassive as evidenced by ever increasing current densities. The 0 mV, 100 mV, and 200 mV hybrid tests all presented similar current density values and behavior with time that was characteristic of passive behavior in that the current densities continuously decreased with time, although more rapidly initially.

The PEIS data, taken from the RAW-6(Ni3) hybrid test in pH 3 brine, collectively indicated the -100 mV potentiostatic hold made the alloy electrode surface stable, but without a protective passivation layer. The 0 mV, 100 mV, and 200 mV PEIS data collectively indicated stable surfaces that became more stable with time. The 300 mV PEIS data shows an unstable surface with no passivation that became increasingly active with time.

The E_{Corr} evolution measurements of the RAW-6(Ni3) alloy indicated that E_{Corr} from a -400 mV potential hold would shift from oxidizing to reducing within one hour, but that this would not occur for a -350 mV potential hold (that is, above -350 mV the alloy should be oxidizing). This behavior same potential oxidation/reduction transition potential was observed for two separate RAW-6(Ni3) alloy electrodes. These measured E_{Corr} values were in contrast with observed E_{Corr} evolution from the hybrid test at -100 mV, which saw reducing conditions start during the initial PEIS measurements in the first hour of the potential hold; although the small amplitude potential changes from the PEIS may have altered the E_{Corr} evolution for the hybrid test so the data may not be directly comparable.

Post Exposure SEM

Under examination by SEM, only the hybrid test at the 300 mV hold potential showed a change to its morphology after the testing. Similar to the attack visible on the bare surface alloy SEM characterizations, the attack appears to be localized to the $ZrFe_2$ phase, and potentially preferential to preexisting crevices. The bare surface potentiodynamic scans subjected the alloys to more aggressive oxidative potentials, and the electrodes showed more evidence of pitting/crevice corrosion, with corrosion appearing to focused on the $ZrFe_2$ phase or interphase regions.

Solution analysis

The 300 mV hybrid test was the only one to consistently show increased concentrations of investigated elements in the test solutions over the test duration, and the only one that had a significant increase in Re concentration. In all cases except for the 300 mV test, Cr and Fe had consistent decreases in solution concentrations for all hybrid tests.

Overall Conclusions and Future Recommendations

All of the RAW-6 Ni:Cr variations had similar passive behavior in the acidic and alkaline brines. The RAW-6(Ni3) alloy variation had the largest passive region in the test solutions, and this alloy was then examined more in depth with hybrid testing and solution sampling, the results of which indicated that in the passive region the alloy forms a protective passivation layer and the elements found in the steel phase, that would be responsible for the majority of the Tc sequestration in a full-scale waste form, are not markedly changed.

SEM/EDS provided evidence of corrosion of the high-Z phases responsible for sequestration of the U in a full-scale waste form, but not of localized corrosion of the steel phases, which indicates general uniform corrosion was likely occurring on the steel phases if corrosion was occurring, or

that the oxide passivation layer was protective of the mostly Fe-Cr phase. The alloy held at transpassive potentials experienced localized corrosion in the Zr-Fe phase, with cracks in this phase which may have initiated further corrosion.

It is recommended that future alloy development should focus on improving the $ZrFe_2$ phase to reduce the microcracking that may lead to initiation sites for crevice corrosion and localized attack. It was originally theorized that the levels of Ni used in the trim additions may have reduced this phenomenon, but that was not observed. A study with a wider Ni addition range may prove more definitive.

5.   REFERENCES

Ebert, W. L. (2015). "Test Plan for Materials Representing Alloyed Waste Forms Made with HT9 Cladding, FCRD-MRWFD-2016-000511."

Keiser, D., Abraham, D., Sinkler, W., Richardson, J., McDeavitt, S. (2000). "Actinide distribution in a stainless steel±15 wt% zirconium high-level nuclear waste form." <u>Journal of Nuclear Materials</u> 279: 234-244.

Olson, L. (2012). Formulation of Reference Alloy Waste Form RAW-3, Savannah River National Laboratory Technical Document, SRNL-STI-2012-00534 and FCRD-SWF-2012-000348.

Durability and Degradation of HT9 Based Alloy Waste Forms with Variable Ni and Cr Content
FCRD-MRWFD-2017-000407
SRNL-STI-2016-00719
December 31, 2016

62

6.   APPENDIX 1: Electrochemical Measurement Data

Bare Surface Potentiodynamic Electrochemical Measurement Data

Table 13 Material Identification

Unique material identification label	RAW-6(Ni1)	RAW-6(Ni3)	RAW-6(Ni5)
Identify QA level	Scoping		
Intended use of material	Basic analysis and characterization		
Production date(s)	FY16		
Production location	SRNL		
Principle investigator	Luke Olson		
Radionuclide content (mass %)	None		
Comments by producer	None		
Location of ~500x magnification SEM image of alloy	SRNL hard drive, AWF folder. 100x and 1000x provided in paper. 500x of RAW-6(Ni3) provided in Figure 1		

Table 14 Corrosion Cell Set-Up

	RAW-6(Ni1)				RAW-6(Ni3)				RAW-6(Ni5)			
Unique material identification label	RAW-6(Ni1)				RAW-6(Ni3)				RAW-6(Ni5)			
Identify QA level	Scoping											
Reference electrode used	RHE in tests, potential changed to SCE for most analysis. RHE is pH dependent.											
Counter electrode used	Graphite. 2 x 0.25" graphite rods spaced equidistant from WE (about 2")											
WE surface finish (oxidized, polished to 600 grit…)	1 micron diamond polish											
WE surface area (cm^2)	**0.88**				**0.95**				**0.98**			
WE density (g/cm^3)	7.8				7.9				7.9			
WE equivalent weight	24.8				25.0				25.1			
Non-conductive epoxy used for WE	Epofix											
Identify and describe test generating sample (if analyzing a reacted specimen)	Samples were all freshly polished prior to testing											
Identify calibration of scale(s) used for solution (If current, or date of last calibration)	Sartorious Practum224-1S: 05/05/2016											
Identify standard name of electrolyte solution	pH 3 acidic brine	pH 5 acidic brine	pH 8 alkaline brine	pH 10 alkaline brine	pH 3 acidic brine	pH 5 acidic brine	pH 8 alkaline brine	pH 10 alkaline brine	pH 3 acidic brine	pH 5 acidic brine	pH 8 alkaline brine	pH 10 alkaline brine
Electrolyte temperature (before, after, during, etc…)	20.8	21.3	21.3	20.9	20.8	21.3	21.3	20.9	20.8	21.3	21.3	20.9
Electrolyte Composition	(0.1 mmol H$_2$SO$_4$ + 10 mmol NaCl)/(1 kg H2O) titrated to desired pH	(0.1 mmol NaOH + 10 mmol NaCl)/(1 kg H2O) titrated to desired pH			(0.1 mmol H$_2$SO$_4$ + 10 mmol NaCl)/(1 kg H2O) titrated to desired pH		(0.1 mmol NaOH + 10 mmol NaCl)/(1 kg H2O) titrated to desired pH		(0.1 mmol H$_2$SO$_4$ + 10 mmol NaCl)/(1 kg H2O) titrated to desired pH		(0.1 mmol NaOH + 10 mmol NaCl)/(1 kg H2O) titrated to desired pH	
Test specific electrolyte conditions	-100x concentration made from 5.8432g NaCl and 100.02g H2O saturated in Air. Solution made (03/07/2016) then used for all tests. -700.00 g of solution used for all tests.											
Test order (Date)	3/07/2016	3/08/2016	3/10/2016	3/09/2016	3/07/2016	3/08/2016	3/10/2016	3/09/2016	3/07/2016	3/08/2016	3/10/2016	3/09/2016

Durability and Degradation of HT9 Based Alloy Waste Forms with Variable Ni and Cr Content
FCRD-MRWFD-2017-000407
SRNL-STI-2016-00719
December 31, 2016

64

Hybrid Testing Electrochemical Measurement Data

Table 15 Corrosion Cell Set-Up

Unique material identification label	RAW-6(Ni3)				
Identify QA level	Scoping				
Reference electrode used	RHE in tests, potential changed to SCE for most analysis. RHE is pH dependent.				
Counter electrode used	Graphite. 2 x 0.25" graphite rods spaced equidistant from WE (about 2")				
WE surface finish (oxidized, polished to 600 grit…)	1 micron diamond polish				
WE surface area (cm$^{2)}$	**1.02**	**1.00**	**1.06**	**1.08**	**1.05**
WE density (g/cm^3)	7.9				
WE equivalent weight	25.0				
Non-conductive epoxy used for WE	Epofix				
Identify and describe test generating sample (if analyzing a reacted specimen)	-100 mV Potentiostatic hold for up to 1 week	0 mV Potentiostatic hold for up to 1 week	100 mV Potentiostatic hold for up to 1 week	200 mV Potentiostatic hold for up to 1 week	300 mV Potentiostatic hold for up to 1 week
Identify calibration of scale(s) used for solution (If current, or date of last calibration)	Sartorious Practum224-1S: 05/05/2016				
Identify standard name of electrolyte solution	pH 3 acidic brine				
Electrolyte temperature (before, after, during, etc…)	21.0	20.3	20.9	19.6	20.7
Electrolyte Composition	(0.1 mmol H$_2$SO$_4$ + 10 mmol NaCl)/(1 kg H2O) titrated to desired pH 3				
Test specific electrolyte conditions	-100x concentration made from 5.8432g NaCl and 100.02g H2O saturated in Air. Solution made (03/07/2016) then used for all tests. -700.00 g of solution used for all tests.				
Test order (Date)	06/16/2016	07/27/2016	06/16/2016	07/27/2016	06/16/2016

Table 16 Solution Sample Data

Vial Sample #	Greene cell origin	tare weight	solution volume	Date sample taken	Time sample taken: military time (hr:min:sec, use cpu time)	final weight	pH (measured 06/28/2016 for 1-12, and 07/13/2016 for 13-20)
1	pot 1	11.7001	5 mL	6/20/2016	11:42:00	16.6056	3.18
2	pot 2	11.7995	5 mL	6/20/2016	11:42 AM	16.5491	3.11
3	pot 3	11.8162	5 mL	6/20/2016	11:42 AM	16.6513	3.15
4	pot 1	11.7612	5 mL	6/21/2016	9:24 AM	16.4752	3.33
5	pot 2	11.7548	5 mL	6/21/2016	9:25 AM	16.4642	3.56
6	pot 3	11.7272	5 mL	6/21/2016	9:26 AM	16.5076	3.52
7	pot 1	11.8078	5 mL	6/23/2016	8:40 AM	16.7166	3.51
8	pot 2	11.8572	5 mL	6/23/2016	8:42 AM	16.6373	4.72
9	pot 3	11.8028	5 mL	6/23/2016	8:43 AM	16.4704	5.3
10	pot 1	11.8404	5 mL	6/27/2016	8:43 AM	16.7898	4.02
11	pot 2	11.7474	5 mL	6/27/2016	8:45 AM	16.6475	5.35
12	pot 3	11.7502	5 mL	6/27/2016	8:46 AM	16.421	6.53
13	pot 1	11.7687	5 mL	7/5/2016	4:51 PM	16.8572	3.18
14	pot 2	11.8054	5 mL	7/5/2016	4:51 PM	16.5933	3.23
15	pot 1	11.7499	5 mL	7/6/2016	2:01 PM	16.438	3.3
16	pot 2	11.7807	5 mL	7/6/2016	2:03 PM	16.5764	3.54
17	pot 1	11.8442	5 mL	7/8/2016	2:47 PM	16.6775	3.39
18	pot 2	11.7973	5 mL	7/8/2016	2:50 PM	16.7507	4.48
19	pot 1	11.7875	5 mL	7/12/2016	11:20 AM	16.8757	3.66
20	pot 2	11.7315	5 mL	7/12/2016	11:22 AM	16.6492	6.11

Durability and Degradation of HT9 Based Alloy Waste Forms with Variable Ni and Cr Content
FCRD-MRWFD-2017-000407
SRNL-STI-2016-00719
December 31, 2016

66

E_{Corr} Evolution Electrochemical Measurement Data

Table 17 Corrosion Cell Set-Up

Unique material identification label	RAW-6(Ni3)	
Identify QA level	Scoping	
Reference electrode used	RHE in tests, potential changed to SCE for most analysis. RHE is pH dependent.	
Counter electrode used	Graphite. 2 x 0.25" graphite rods spaced equidistant from WE (about 2")	
WE surface finish (oxidized, polished to 600 grit…)	1 micron diamond polish	
WE surface area (cm^2)	**1.00**	**1.06**
WE density (g/cm^3)	7.9	
WE equivalent weight	25.0	
Non-conductive epoxy used for WE	Epofix	
Identify and describe test generating sample (if analyzing a reacted specimen)	2 min at -500 mV vs SCE, then move oxidative 50 mV, holding at each step for 1 hour, until reaching 150 mV vs SCE	
Identify calibration of scale(s) used for solution (If current, or date of last calibration)	Sartorious Practum224-1S: 05/05/2016	
Identify standard name of electrolyte solution	pH 3 acidic brine	
Electrolyte temperature (before, after, during, etc…)	20.8	21.3
Electrolyte Composition	(0.1 mmol H$_2$SO$_4$ + 10 mmol NaCl)/(1 kg H2O) titrated to desired pH 3	
Test specific electrolyte conditions	-100x concentration made from 5.8432g NaCl and 100.02g H2O saturated in Air. Solution made (03/07/2016) then used for all tests. -700.00 g of solution used for all tests.	
Test order (Date)	07/28/2016	